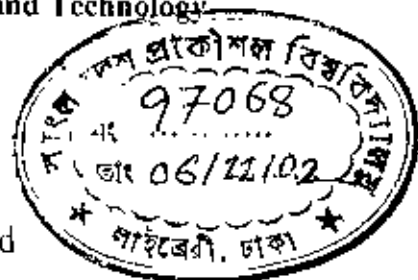# Conjugate effect of conduction and convection with natural convection flow from a vertical flat plate and in an inclined square cavity

A dissertation submitted in partial fulfillment of the requirements for the award of the degree

of
Master of Philosophy
in Mathematics

By
MD. ZAFAR IQBAL KHAN
Registration no. 9509001, Session 1994-95-96
Department of Mathematics
Bangladesh University of Engineering and Technology
Dhaka-1000

Supervised & approved

By
A. K. Hazra
Department of Mathematics, BUET

Co-supervised & approved

By
Prof. M. A. Hossain
Department of Mathematics, D.U

Bangladesh University of Engineering and
Technology, Dhaka-1000

Conjugate effect of conduction and convection with natural convection flow from a vertical flat plate and in an inclined square cavity

A dissertation submitted in partial fulfillment of the

requirement for the award of the degree

of

Master of Philosophy

By
MD. ZAFAR IQBAL KHAN
Registration no. 9509001, Session 1994-95-96
Department of Mathematics
Bangladesh University of Engineering and Technology
Dhaka-1000

The Thesis Entitled

Conjugate effect of conduction and convection with natural convection flow from a vertical flat plate and in an inclined square cavity
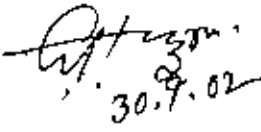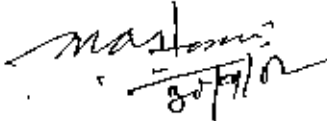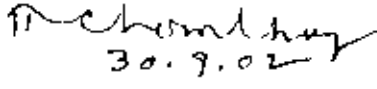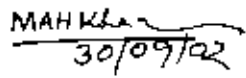
Submitted By
MD. ZAFAR IQBAL KHAN

Registration no. 9509001, Session 1994-95-96, a part time student of M. Phil
(Mathematics) has been accepted as satisfactory in partial fulfillment for the   .

Degree of

Master of Philosophy in Mathematics

on September, 2002.

Board of Examiners

1. A. K. Hazra
    Associate Professor
    Department of Mathematics,   Supervisor
    BUET. Dhaka-1000

2. Dr. M. A. Hossain
    Professor
    Department of Mathematics,   Co-supervisor
    University of Dhaka, Dhaka-1000

3. Head
    Department of Mathematics   Member
    BUET, Dhaka-1000   (Ex-officio)

4. Dr. Md. Abdul Hakim Khan
    Assistant Professor
    Department of Mathematics   Member
    BUET, Dhaka-1000

5. Dr. G. D. Roy
    Professor
    Department of Mathematics,   Member
    SUST, Sylhet   (External)

Table of Contents

Abstract

In this thesis, the thermo-fluid-dynamic field resulting from the coupling of natural convection along and conduction inside a heated flat plate is numerically studied by means of implicit finite difference method in the entire region starting from the lower part of the plate to down stream. The results in terms of shear stress coefficient and surface temperature coefficient for different Prandtl numbers are compared with the perturbation solution near the lower part of the plate and asymptotic solution in the down stream region and found an excellent agreement for flat plate. In second part unsteady laminar natural convection flow has been considered in an inclined square cavity. The top horizontal wall, the right vertical wall , the bottom wall of the cavity are cool and the left vertical wall is heated. The equations are non-dimensional and solved numerically by an upwind finite difference method together with a successive over-relaxation (SOR) technique. Results are shown on the streamlines configuration as well as the isolines of temperatures. The fluid has Prandtl number Pr =7.0 while the value of the Rayleigh number, Ra varies from 10^3 to 10^7 and coupling parameter, p varies from 0.0 to 1.0 and angle inclination ϕ, varies from 0^0 to 90^0 for cavity.

CANDIDATE'S DECLARATION

I hereby declare that the work which is being presented in the thesis entitled "Conjugate effect of conduction and convection with natural convection flow from a vertical flat plate and in an inclined square cavity" submitted in partial fulfillment of the requirements for the award of the degree of Master of Philosophy in Mathematics, in the department of Mathematics, Bangladesh University of Engineering and Technology, Dhaka is an authentic record of my own work.

The matter presented in this thesis has not been submitted by me for the award of any other degree in this or any other University.

Date: September 30, 2002

(Md. Zafar Iqbal Khan)

Acknowledgement

Nomenclature

x	Streamwise coordinate	ψ	Stream function
y	Transverse coordinate	ν	Kinematic viscosity
u	Velocity component in the x-direction	ρ	Fluid density
v	Velocity component in the y-direction	μ	Viscosity of the fluid
f	Dimensionless stream function	b	Plate thickness
g	Acceleration due to gravity	d	$(T_b - T_\infty)/T_\infty$
T	Temperature of the fluid	l	Length of the plate
T_b	Temperature at outside of the plate	κ_s	Thermal conductivity of the ambient solid
T_∞	Temperature of the ambient fluid	κ_f	Thermal conductivity of the ambient fluid
T_{sa}	Solid temperature	θ	Dimensionless temperature $(T - T_\infty)/(T_b - T_\infty)$
C_p	Specific heat	L	Reference length , $\nu^{2/3}/g^{1/3}$
Pr	Prandtl number	p	Coupling parameter
Ra	Rayleigh number		

List of tables

List of Figures

Chapter 1

Introduction

It is well established that when convective heat transfer results are strongly dependent on thermal boundary conditions, consideration of convective heat transfer problems as conjugated problems is necessary to obtain physically more strict results. Many research efforts have been given to the conjugate problems of forced convection heat transfer both experimental and theoretical but few works have been devoted to the conjugate problem of free convection. Gdalevich and Fertman [1] stated conclusively that the use of numerical method for solving the initial system of governing partial differential equation such as finite difference methods, is evidently the most promising in studies of conjugate free convection.

According to Kelleher and Yang [2] the analytical treatments used extensively in conjugate forced convection problems are difficult due to matching a non-linear solution of free convection in a fluid with linear conduction solution in a solid body at the solid fluid interface. Successful analytical solution for the problem of conjugate free convection about tapered, downward projection fin of a simple power low form is obtained by Lock and Gunn [3]. Chida and Katto [4] studies the conjugate problems in this direction by the use of the vertical dimensional analysis. They applied their method to the interpretation of previously studied conjugate heat transfer problems. When convective heat transfer depends strongly on the thermal boundary conditions, natural convection must be studied as a mixed problem if one needs accurate analysis of the thermo-fluid-dynamic field that pointed by Miyamoto et-al [5]. They analyzed the relative importance of the parameters of the problem with reference with axial heat conduction. Timma and Padet [6] by extending the analysis of Gosse [7] have developed a technique which improves the results given by the first term of asymptotic solution of the problem. In the same work a new correlation for the evaluation of heat transfer

1

coefficient had also been presented. This analysis holds for high value of the abscissa x, the value of the point x_0 from which the expansion is valid depends on the parameters that govern the problem.

Coupled natural convection evaluating by the region which the point x_0 falls in, has been made by Pozzi and Lupo [8] improving the results concerning the asymptotic expansion by adding terms of higher order with respect to the first one discussed the general form of the asymptotic expansions which is singular for the presence of eigen solutions and determined the expansion holding for small values of x in an accurate way, by taking into account many terms of the series by means of Padé approximant techniques.

Less work has been carried out for more complex thermal boundary conditions, such as an imposed thermal gradient that is neither purely horizontal nor purely vertical. Shiralkar and Tien [16] investigated numerically natural convection in an enclosure with temperature gradients imposed in both the horizontal and vertical directions simultaneously. Chao and Ozoe [16] investigated the problem of natural convection in an inclined box with half the bottom surface heated and half insulated, while the top surface was cooled. Anderson and Lauriat [18] analyzed experimentally as well as theoretically the natural convection due to one isothermal cold vertical wall and a hot bottom wall. Kimura and Bejan [19] studied numerically the convection flow in a rectangular enclosure with the entire lower surface cooled and one of the vertical walls heated. November and Nansteel [20] and Nicolas and Nansteel [21] performed experiments and numerical investigations on convection in a water filled enclosure with a single cold isothermal vertical wall and a partially heated bottom wall. Ganzarolli and Milanez [22] computed the case of a heated bottom wall and isothermally cooled vertical walls. Recently, Velusamy et al. [23] investigated the steady two-dimensional natural convection flow in a rectangular enclosure with a linearly-varying surface temperature on the left vertical wall, cooled right vertical and top walls and a uniformly-heated bottom wall. In this latter investigation, mild natural

convection was found to reduce the heat load to the cold walls and for any value of aspect ratio it was also found that there exists a critical Rayleigh number for which heat load is a minimum.

In early works on flow in porous media, the Darcy law has been used which is applicable to slow flows and does not account for inertial and boundary effects (termed as non-Darcy effects). These effects are important when the flow velocity is relatively high and in the presence of a boundary, as reported first by Vafai and Tien [24]. Recently, Khanafer and Chamkha [25] investigated numerically the Brinkman-extended Darcy unsteady mixed convection flow in an enclosure, with internal heat generation and with inclusion of the convective terms in the governing equations, using the control volume method by Patankar [26].

In the present work we have used to give further contribution to the study of coupled natural convection by introducing new transformation to the problem posed by Pozzi et al. [8] that leads the solution for x raising between 0 to ∞ that is solution near the leading edge to down stream region at the vertical surface in Chapter 2. Lastly unsteady laminar natural convection flow has been considered in an inclined square cavity in Chapter 3. The equations are non-dimensionalized and solved numerically by an upwind finite difference method together with a successive over relaxation (SOR) technique developed by Hossain and Rees [27].

Chapter 2

Coupling of conduction with natural convection flow from a
vertical flat plate

2.1 Introduction

In this chapter the thermo-fluid-dynamic field resulting from the coupling of
natural convection along and conduction inside a heated flat plate is studied by
means of implicit finite difference method in the entire region starting from the
lower part of the plate to downstream. The results in terms of shear stress
coefficient and surface temperature coefficient for different Prandtl numbers are
compared with the perturbation solution near the lower part of the plate and
asymptotic solution in the down stream region and found an excellent agreement.

2.2 Governing equations of the flow

We describe the steady two-dimensional flow due to free convection flow along a
side of a vertical flat plate of thickness b insulated on the edges with a temperature
T_b maintained on the other side (Fig 2.1).

The thermo-fluid-dynamic field in the fluid is governed by the boundary layer
equations are

$$\frac{\partial u}{\partial x} + \frac{\partial v}{\partial y} = 0 \tag{2.1}$$

$$u\frac{\partial u}{\partial x} + v\frac{\partial u}{\partial y} = v_f \frac{\partial^2 u}{\partial y^2} + g\beta(T - T_\infty) \tag{2.2}$$

$$u\frac{\partial T}{\partial x} + v\frac{\partial T}{\partial y} = \frac{\kappa_f}{\rho c_p}\frac{\partial^2 T}{\partial y^2} \tag{2.3}$$

4
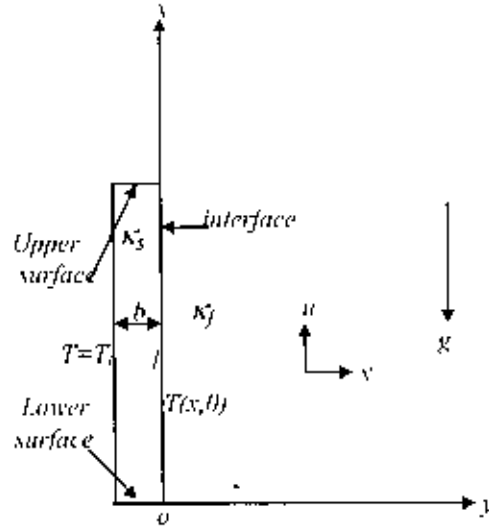
Fig. 2.1: A vertical flat plate and the coordinate system

where u and v are the velocity components along the x and y directions respectively, T is the temperature of the fluid, T_∞ and T_b are the temperature of the ambient fluid and outside the plate respectively, g is the gravitational acceleration, β is the volumetric coefficient of thermal expansion, v is the kinematic viscosity, ρ is the density , κ_f is the thermal conductivity of the ambient fluid, c_p is the specific heat at constant pressure.

The boundary conditions to be satisfied by the above equations are

$u = 0, v = 0 \quad$ at $y = 0$

$u = 0, T = T_\infty$ at $y = \infty$ (2.4a)

The coupling conditions require that temperature and heat flux be continuous at the interface. At the interface

$$\kappa_s \frac{\partial T_{so}}{\partial y} = \kappa_f \left(\frac{\partial T}{\partial v} \right)_{v=0}$$ (2.4b)

where κ_s and κ_f is the thermal conductivity of the solid and fluid respectively. T_{so} the temperature in the solid as given by Miyamoto et. al [5] is

$$T_{so} = T(x,0) - [T_b - T(x,0)]\frac{y}{b}$$ (2.4c)

5

where $T(x,0)$ is the unknown temperature at the interface to be determined from the solutions of equations.

2.3 Transformation of the governing equation

We introduce the following dimensionless dependent and independent variables:

$$\bar{x} = \frac{x}{L}, \quad \bar{y} = \frac{y}{L} d^{1/4}, \quad u = \frac{\nu}{L} d^{1/2} \bar{u}, \quad v = \frac{\nu}{L} d^{1/4} \bar{v}, \quad \frac{T - T_\infty}{T_b - T_\infty} = \theta,$$

$$L = \frac{\nu^{2/3}}{g^{1/3}}, \quad d = \beta(T_b - T_\infty) \tag{2.5}$$

Using the above dimensionless variables into the equations (2.1)-(2 3) we get the following dimensionless equations:

$$\frac{\partial u}{\partial x} + \frac{\partial v}{\partial y} = 0 \tag{2.6}$$

$$u\frac{\partial u}{\partial x} + v\frac{\partial u}{\partial y} = \frac{\partial^2 u}{\partial y^2} + \theta \tag{2.7}$$

$$u\frac{\partial \theta}{\partial x} + v\frac{\partial \theta}{\partial y} = \frac{1}{Pr}\frac{\partial^2 \theta}{\partial y^2} \tag{2.8}$$

where $Pr = \mu c_p/\kappa$, the Prandtl number.

The corresponding boundary conditions (2.4a,b,c) take the form

$$u = v = 0, \; \theta - 1 = p\frac{\partial \theta}{\partial y} \quad \text{at } y = 0$$

$$u = \theta = 0 \quad \text{at } y = \infty \tag{2.9}$$

where $p = (\kappa_f/\kappa_s)(b/L)d^{1/4}$, the coupling parameter.

The problem described here is governed by the coupling parameter p, the order of magnitude of which depends essentially on b/L and κ_f/κ_s, $d^{1/4} = O(1)$. As L is small, b/L is very large. When the fluid is air $\kappa_f/\kappa_s \ll 1$ if this plate is highly conductive i.e., $\kappa_s \gg 1$ and reach the order of 0.1 for materials such as glass. Therefore p is in many cases, but not always, a small number. Briefly in the present investigation we have considered $p = 1$ which is accepted for b/L of $O(\kappa_f/\kappa_s)$.

According to Pozzi and Lupo [8], for the downstream and upstream regimes, we introduced the following transformations :

$$\psi = x^{3/4} f(x,\eta), \quad \eta = yx^{-1/4}, \quad \theta = g \tag{2.10}$$

and

$$\psi = x^{4/5} F(x,\eta) \quad \eta = yx^{-1/5}, \quad \theta = x^{1/5} G \tag{2.11}$$

respectively. Here ψ is the stream function that satisfies the equation of continuity and η is pseudo-similarity variable and

$$u = \frac{\partial \psi}{\partial y}, \quad v = -\frac{\partial \psi}{\partial x}$$

Combining the transformations given by (2.10) and (2.11) following generalized transformation for the flow region starting from upstream to downstream can be determined. The new transformations are as follows:

$$\psi = x^{4/5}(1+x)^{-1/20} f(\eta, x), \quad \eta = yx^{-1/5}(1+x)^{-1/20}, \quad \theta = x^{1/5}(1+x)^{-1/5} h \tag{2.12}$$

Here h is the dimensionless temperature.

Using transformations (2.12) in (2.7)-(2.8) we get

$$f''' + \frac{16+15x}{20(1+x)} ff'' - \frac{6+5x}{10(1+x)} f'^2 + h = x\left(f' \frac{\partial f'}{\partial x} - f'' \frac{\partial f}{\partial x} \right) \tag{2.13}$$

$$\frac{1}{\Pr} h'' + \frac{16+15x}{20(1+x)} fh' - \frac{1}{5(1+x)} f'h = x\left(f' \frac{\partial h}{\partial x} - h' \frac{\partial f}{\partial x} \right) \tag{2.14}$$

In the above equations the primes denote differentiation with respect to η

Boundary conditions (2.9) then take the following form

$$f(x,0) = f'(x,0) = 0, \quad h'(x,0) = -(1+x)^{1/4} + x^{1/5}(1+x)^{1/20} h(x,0)$$
$$f'(x,\infty) = 0, h(x,\infty) = 0 \tag{2.15}$$

2.4 Methods of Solution

To find the solutions of the equations (2.13) and (2.14) along with the boundary condition (2.15) we consider three different cases namely (i) series solution for small x; (ii) series solution for large x; (iii) finite difference technique(see

7

appendix) for all x for different values of Prandtl number Pr while the coupling parameter $p=1$. In order to compare the present results with Pozzi and Lupo [8] for small and large values of x, we discuss the method of solutions in details.

2.4.1 Solution for small x

For small x, we obtained

$(16+15x)/20(1+x) \rightarrow 4/5$, $(6+5x)/10(1+x) \rightarrow 3/5$, $1/5(1+x) \rightarrow 1/5$

and $-(1+x)^{1/4} + x^{1/5}(1+x)^{1/20} \rightarrow -1 + x^{1/5}$

Then equations (2.13) and (2.14) reduces to

$$f''' + \frac{4}{5}ff'' - \frac{3}{5}f'^2 + h = x\left(f'\frac{\partial f'}{\partial x} - f''\frac{\partial f}{\partial x}\right) \tag{2.16}$$

$$\frac{1}{Pr}h'' + \frac{4}{5}fh' - \frac{1}{5}f'h = x\left(f'\frac{\partial h}{\partial x} - h'\frac{\partial f}{\partial x}\right) \tag{2.17}$$

and boundary conditions reduces to

$$f(x,0) = f'(x,0) = 0, h'(x,0) = -1 + x^{1/5}h,$$
$$f'(x,\infty) = h(x,\infty) = 0 \tag{2.18}$$

Since x is small, we may expand the functions $f(x,\eta)$ and $h(x,\eta)$ in powers of $x^{1/5}$ as given below:

$$f(x,\eta) = \sum_{i=0}^{\infty} x^{i/5} f_i(\eta) \text{ and } h(x,\eta) = \sum_{i=0}^{\infty} x^{i/5} h_i(\eta) \tag{2.19}$$

Now, substituting the expansions (2.19) into equations (2.16)-(2.17) and boundary condition (2.18) and taking the terms $O(x^0)$ and $O(x^{n/5})$ respectively we get

$$f_0''' + \frac{4}{5}f_0 f_0'' - \frac{3}{5}f_0'^2 + h_0 = 0 \tag{2.20}$$

$$\frac{1}{Pr}h_0'' + \frac{4}{5}f_0 h_0' - \frac{1}{5}f_0' h_0 = 0 \tag{2.21}$$

$$f_0(0) = f_0'(0) = 0, h_0'(0) = -1$$
$$f_0'(\infty) = 0, h_0(\infty) = 0 \tag{2.22}$$

8

and

$$f_n''' + \frac{4}{5}\sum_{k=0}^{n} f_k f_{n-k}'' - \frac{3}{5}\sum_{k=0}^{n} f_k' f_{n-k}' + h_k = \sum_{k=1}^{n}\frac{k}{5}\left(f_{n-k}' f_k' - f_{n-k}'' f_k\right)$$

(2.23)

$$\frac{1}{\mathrm{Pr}}h_n'' + \frac{4}{5}\sum_{k=0}^{n} f_k h_{n-k}' - \frac{1}{5}\sum_{k=0}^{n} f_{n-k}' h_k = \sum_{k=1}^{n}\frac{k}{5}\left(f_{n-k}' h_k - h_{n-k}' f_k\right)$$

(2.24)

$$f_n(0) = f_n'(0) = 0, h_n' = h_{n-1}(n > 0)$$
$$f_n'(\infty) = 0, \ h_n(\infty) = 0$$

(2.25)

Equations (2.20)-(2.21) with boundary condition (2.22) are coupled and nonlinear that had already been integrated by Sparrow and Gregg [10] for the natural convection flow from vertical flat plate with uniform surface heat flux with little difference in the coefficients. We obtain the solutions using the method of iteration developed by Nachtsheim and Swigert [14] for different values of the Prandtl number. Subsequent equations for $n = 1, 2, 3, \ldots$ are coupled and with non-homogeneous boundary conditions nontrivial solutions of which can be obtained easily using the aforementioned method. Here we have obtained the solutions for $n = 10$. Numerical values of $f_i''(0)$ and $\theta_i(0)$ thus obtained are compared with Pozzi and Lupo [8] side by side in Table 2.1 and Table 2.2 respectively. The careful observation shows excellent agreement between these two results.

After knowing the values of the functions $f(\eta,x)$, $h(\eta,x)$ and their derivatives we can calculate the values of the skin friction coefficient $f''(0,x)$ and the surface temperature co-efficient $\theta(0, x)$ in the region near the point of leading edge from the following relations:

$$f''(0,x) = x^{2/5}\left(f_0''(0) + x^{1/5} f_1''(0) + x^{2/5} f_2''(0) + x^{3/5} f_3''(0) + \ldots\right)$$

(2.26a)

$$\theta(0,x) = x^{1/5}\left(h_0(0) + x^{1/5} h_1(0) + x^{2/5} h_2(0) + x^{3/5} h_3(0) + \ldots\right)$$

(2.26b)

Numerical values obtained from the above expression for $f''(0,x)$ and $\theta(0,x)$ are shown graphically in Fig. 2.2 and Fig. 2.3 respectively for different values of x as well as Pr. The broken curves for smaller values of x are the representations of

these solutions. The comparison of these curves with the solids that are obtained by the finite difference are found in excellent agreement.

2.4.2 Solutions for large x

For large x, we get

$(16+15x)/20(1+x) \to 3/4$, $(6+5x)/10(1+x) \to 1/2$, $1/5(1+x) \to 0$

and $h'(x,0) = -(1+x)^{1/4} + x^{1/5}(1+x)^{1/20} h(x,0) \to h(x,0) = 1 + x^{-1/4} h'(x,0)$

Then equations (2.13) and (2.14) reduces to

$$f''' + \frac{3}{4} ff'' - \frac{1}{2} f'^2 + h = x\left(f' \frac{\partial f'}{\partial x} - f'' \frac{\partial f}{\partial x} \right) \tag{2.27}$$

$$\frac{1}{\Pr} h'' + \frac{3}{4} fh' = x\left(f' \frac{\partial h}{\partial x} - h' \frac{\partial f}{\partial x} \right) \tag{2.28}$$

Corresponding boundary conditions then take the form

$$f(x,0) = f'(x,0) = 0,\ h(x,0) = 1 + x^{-1/4} h'(x,0)$$
$$f'(x,\infty) = h(x,\infty) = 0 \tag{2.29}$$

Since x is large, solutions of the equations (2.27)-(2.28) with boundary condition (2.29) may be obtained by using the perturbation method. We expand the functions $f(x,\eta)$ and $h(x,\eta)$ in powers of $x^{-1/4}$ as given below:

$$f(x,\eta) = \sum_{i=0}^{\infty} x^{-i/4} f_i(\eta) \text{ and } h(x,\eta) = \sum_{i=0}^{\infty} x^{-i/4} h_i(\eta) \tag{2.30}$$

Now substituting the expansions (2.30) in equations (2.27)-(2.28) with boundary condition and taking the terms $O(x^0)$ and $O(x^{-n/4})$ we get

$$f_0''' + \frac{3}{4} f_0 f_0'' - \frac{1}{2} f_0'^2 + h_0 = 0 \tag{2.31}$$

$$\frac{1}{\Pr} h_0'' + \frac{3}{4} f_0 h_0' = 0 \tag{2.32}$$

$$f_0(0) = f_0'(0) = 0, h_0(0) = 1$$
$$f_0'(\infty) = 0,\ h_0(\infty) = 0 \tag{2.33}$$

and

$$f_n''' + \frac{3}{4}\sum_{k=0}^{n} f_k f_{n-k}'' - \frac{1}{2}\sum_{k=0}^{n} f_k' f_{n-k}' + h_n = \sum_{k=1}^{n}\frac{k}{4}\left(f_{n-k}'' f_k - f_{n-k}' f_k'\right) \tag{2.34}$$

$$\frac{1}{\Pr}h_n'' + \frac{3}{4}\sum_{k=0}^{n} f_k h_{n-k}' = \sum_{k=1}^{n}\frac{k}{4}\left(h_{n-k}' f_k - f_{n-k}' h_k\right) \tag{2.35}$$

$$f_n(0) = f_n'(0) = 0, h_n = h_{n-1}'\,(n > 0)$$
$$f_n'(\infty) = 0,\ h_n(\infty) = 0 \tag{2.36}$$

Equations (2.31)-(2.32) along with the boundary conditions (2.33) represent the similarity equations governing the natural convection flow from a vertical heated surface maintained at uniform temperature that had first been investigated by Pohlhausen and Schmidt [11,12]. As before, these equations also differ only with the coefficients with those deduced by the aforementioned authors. However for comparison purpose here also we implement the Nachtsheim and Swigert [14] iteration technique in finding the solutions for different values of the Prandtl number. As before, here also we apply the same method, unlike the eigenvalue solution obtained by Pozzi and Lupo [8], in finding the solutions of the subsequent sets of equations for $n = 1, 2, 3, \ldots$; since the boundary condition of the above equations are non-homogeneous and we obtained non-trivial solutions easily. In Table 2.3 and Table 2.4 numerical values of the functions $f_i''(0)$ and $\theta_i(0)$ (for $i=1,2$ and 3) are shown for different values of the Prandtl number along with those obtained by Pozzi and and Lupo [8]. Here also the comparison between these two results are found an excellent agreement.

Finally knowing the values of the functions $f(\eta,x)$ and $h(\eta,x)$ and their derivatives we can calculate the values of the skin friction coefficient and surface temperature for large values of x in the region where the flow is dominated only by the buoyancy force:

$$f''(0,x) = f_0''(0) + x^{-1/4} f_1''(0) + x^{-2/4} f_2''(0) + x^{-3/4} f_3''(0) + \ldots \tag{2.37a}$$

and

$$\theta(0, x) = h_0(0) + x^{-1/4} h_1(0) + x^{-2/4} h_2(0) + x^{3/4} h_3(0) + \ldots \qquad (2.37\mathrm{b})$$

In Fig. 2.2 and Fig. 2.3 numerical values of $f''(x, 0)$ and $\theta(x, 0)$ are depicted and compared with the finite difference solutions. It can be seen that the curves shown from these solutions are over lapping with those of the finite difference at large values of x that implies that both the solutions are in excellent agreement. Velocity and temperature profiles are shown in Fig 2.3 and Fig 2.4.

2.5 Results and discussion

If we know the values of the functions $f(\eta, x)$, $h(\eta, x)$ and their derivatives for different values of the Prandtl number Pr, we may calculate the numerical values of the surface temperature $\theta(0, x)$ and the velocity gradient $f''(0, x)$ at the surface that are important from the physical point of view. Numerical values of $\theta(0, x)$ are obtained from the following relations,

$$\theta(0, x) = x^{1/5} (1+x)^{-1/5} h(x, 0)$$

Numerical value of the velocity gradient $f''(0, x)$ and the surface temperature $\theta(0, x)$ are depicted graphically in Fig. 2.2 and Fig. 2.3 against the axial distance x in the interval $[0, 10]$ for the values the Prandtl number Pr = 0.73, 1.97 and 2.97 that had been taken into account by Pozzi and Lupo [8] in their analyses. Fig. 2.2 shows that an increase of Prandtl number leads to decrease of the value of shear stress coefficient $f''(0, x)$ as well as the surface temperature $\theta(0, x)$.

In Fig. 2.4 and Fig. 2.5 numerical value of velocity profile $f'(\eta, x)$ and temperature profile $\theta(\eta, x)$ are depicted against the similarity variable η in $[0,8]$ are shown graphically for values of the Prandtl number Pr = 0.73, 1.97 and 2.97. In the above figures effect of the axial distance are also shown. To show its effect on the velocity and the temperature profiles in the boundary layer regimes value of x are chosen to be 1.05 and 3.33 which are represented by solid and broken curves respectively. From Fig.2.4 and Fig.2.5 we observe that both velocity and

temperature profiles decrease owing to increase in the value of the Prandtl number. We may also observe that an increase in the value of the axial distance x leads to decrease in both the velocity and the temperature profiles.

2.6 Conclusions:

We have studied to the study of coupled natural convection and conduction in a flat plate introducing a new class of transformation that leads the solution to the regime near the leading edge to down stream regime along the vertical surface. The coupling of conduction required that the temperature and the heat flux be continuous at the interface. The equations are integrated using the implicit finite difference method and the results are found to be an excellent agreement with the corresponding asymptotic solution. We may thus conclude that the present strained coordinate transformations yield appropriate equations which provide more accurate result than the perturbation solutions.

Table 2.1 Initial expansion : values of $f_n''(0)$ for comparison

	Pr = 0.733		Pr = 2.97	
	Present	Pozzi et al	Present	Pozzi et al
0	1.537	1.540	9.190×10^{-1}	9.197×10^{-1}
1	−1.646	−1.641	-6.822×10^{-1}	-6.799×10^{-1}
2	1.624	1.624	4.704×10^{-1}	4.698×10^{-1}
3	−1.370	−1.371	-2.787×10^{-1}	-2.787×10^{-1}
4	9.445×10^{-1}	9.453×10^{-1}	1.359×10^{-1}	1.360×10^{-1}
5	-4.834×10^{-1}	-4.840×10^{-1}	-4.981×10^{-2}	-4.992×10^{-2}
6	1.209×10^{-1}	1.210×10^{-1}	9.43×10^{-3}	9.470×10^{-3}
7	7.296×10^{-2}	7.296×10^{-2}	3.30×10^{-3}	3.295×10^{-3}
8	-1.091×10^{-1}	-1.095×10^{-1}	-3.88×10^{-3}	-3.895×10^{-3}
9	5.675×10^{-2}	5.699×10^{-2}	1.56×10^{-3}	1.570×10^{-3}
10	7.51×10^{-3}	7.548×10^{-3}	3.0×10^{-5}	3.10×10^{-5}

Table 2.2 Initial expansion: values of $\theta_n(0)$ for comparison

n	Pr=0.733		Pr=2.97	
	Present	Pozzi et al	Present	Pozzi et al
0	2.042	2.042	1.412	1.411
1	−3.085	−3.083	−1.483	−1.481
2	3.791	3.789	1.271	1.271
3	−3.887	−3.886	$−9.153\times10^{-1}$	$−9.147\times10^{-1}$
4	3.323	3.322	5.513×10^{-1}	5.512×10^{-1}
5	−2.296	−2.298	$−2.703\times10^{-1}$	$−2.704\times10^{-1}$
6	1.170	1.172	9.876×10^{-2}	9.896×10^{-2}
7	$−2.848\times10^{-1}$	$−2.853\times10^{-1}$	$−1.817\times10^{-2}$	$−1.827\times10^{-2}$
8	$−1.838\times10^{-1}$	$−1.844\times10^{-1}$	$−6.96\times10^{-3}$	$−6.959\times10^{-3}$
9	2.671×10^{-1}	2.681×10^{-1}	7.84×10^{-3}	7.875×10^{-3}
10	$−1.356\times10^{-1}$	$−1.362\times10^{-1}$	$−3.07\times10^{-3}$	$−3.093\times10^{-3}$

Table 2.3. Asymptotic expansion : values of $f_i''(0)$ for comparison

n	Pr=0.733		Pr=2.97	
	Present	Pozzi et al	Present	Pozzi et al
0	9.532×10^{-1}	9.532×10^{-1}	7.528×10^{-1}	7.522×10^{-1}
1	-2.949×10^{-1}	-2.908×10^{-1}	-3.705×10^{-1}	-3.693×10^{-1}
2	1.143×10^{-1}	1.143×10^{-1}	2.391×10^{-1}	2.392×10^{-1}
3	-4.121×10^{-1}	-4.128×10^{-1}	-1.504×10^{-1}	-1.515×10^{-1}

Table 2.4. Asymptotic expansion : values of $\theta_n(0)$ for comparison

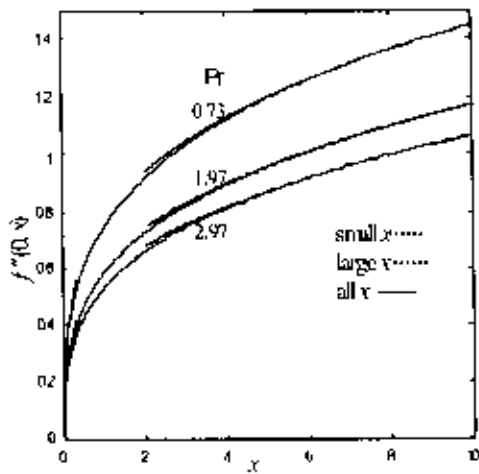| n	Pr=0.733		Pr=2.97	
	Present	Pozzi et al	Present	Pozzi et al
0	-3.610×10^{-1}	-3.591×10^{-1}	-5.745×10^{-1}	-5.749×10^{-1}
1	1.315×10^{-1}	1.315×10^{-1}	3.414×10^{-1}	3.414×10^{-1}
2	-3.616×10^{-2}	-3.593×10^{-2}	-1.547×10^{-1}	-1.545×10^{-1}
3	3.847×10^{-8}	3.845×10^{-8}	8.481×10^{-7}	8.482×10^{-7}

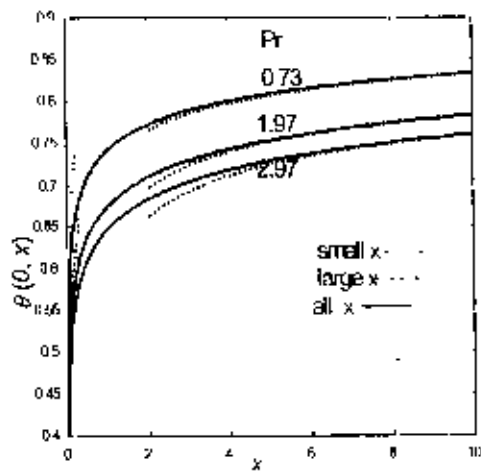Fig. 2.2: Skin friction against axial distance x for different Pr.

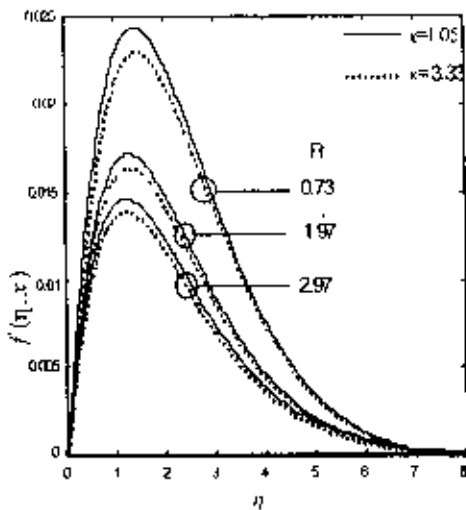Fig. 2.3: Non dimensional temperature against axial distance x for different Pr.

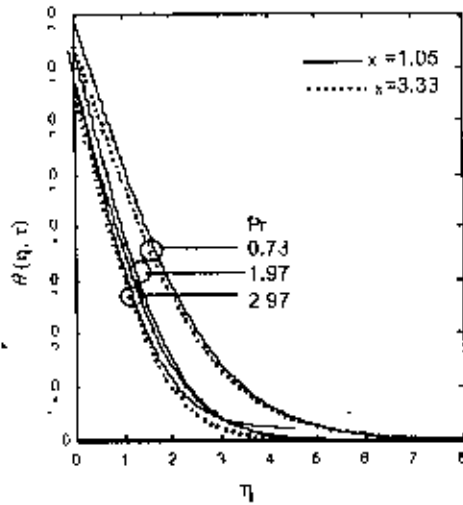Fig. 2.4: Velocity profile against η for different Pr

Fig. 2.5: Temperature profile against η for different Pr

17

Chapter 3

Coupling of conduction with natural convection flow of a fluid in an inclined square cavity

3.1 Introduction

In this chapter unsteady laminar natural convection flow has been considered in an inclined square cavity filled with a fluid. The top horizontal wall , the right vertical wall , the bottom wall of the cavity are cooled and the left vertical wall is heated. The equations are made non-dimensional and solved numerically by an upwind finite difference method together with a successive over-relaxation (SOR) technique. The streamlines and isotherms are presented as well as the rate of heat transfer from walls of the cavity. The fluid has Prandtl number, $Pr = 7.0$ while the value of the Rayleigh number, Ra is from 10^3 to 10^7, angle of inclination, ϕ is from 0^0 to 90^0 and coupling parameter p varies from 0 to 1.

3.2 Governing equations of the flow

we consider an inclined square cavity of height H filed with a fluid as shown in Fig 3.1a. The right, the bottom and the top walls are maintained at a constant cool temperature T_c and the temperature of the left vertical wall is $T_H (T_H > T_c)$ of thickness b and with a temperature T_b maintained on the other side(Fig 3.1a). One must solved the coupled thermal fields in the solid and the fluid.

  We further assume unsteady laminar flow of a viscous incompressible fluid having constant properties. The effect of buoyancy is included through the well-known Boussinesq approximation. Finally, the direction of the gravitational force is as indicated in Fig 3.1a
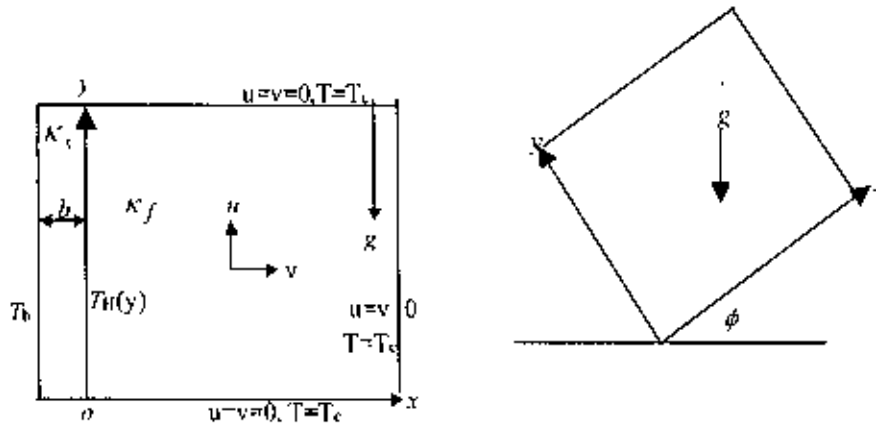
Fig 3.1a: The flow configuration and coordinate system

Under the above assumptions, the conservation equations for mass, momentum and energy in a two- dimensional Cartesian coordinate system are

$$\frac{\partial u}{\partial x} + \frac{\partial v}{\partial y} = 0 \tag{3.1}$$

$$\frac{\partial u}{\partial t} + u\frac{\partial u}{\partial x} + v\frac{\partial u}{\partial y} = -\frac{1}{\rho}\frac{\partial p}{\partial x} + \upsilon\left(\frac{\partial^2 u}{\partial x^2} + \frac{\partial^2 u}{\partial y^2}\right) + g\beta(T - T_c)\sin\phi \tag{3.2}$$

$$\frac{\partial v}{\partial t} + u\frac{\partial v}{\partial x} + v\frac{\partial v}{\partial y} = -\frac{1}{\rho}\frac{\partial p}{\partial y} + \upsilon\left(\frac{\partial^2 v}{\partial x^2} + \frac{\partial^2 v}{\partial y^2}\right) + g\beta(T - T_c)\cos\phi \tag{3.3}$$

$$\frac{\partial T}{\partial t} + u\frac{\partial T}{\partial x} + v\frac{\partial T}{\partial y} = \alpha\left(\frac{\partial^2 T}{\partial x^2} + \frac{\partial^2 T}{\partial y^2}\right) \tag{3.4}$$

where u and v are the fluid velocity components in the x and y direction respectively. T the temperature, p is the fluid pressure, β is the volumetric thermal expansion coefficient, ϕ is the angle and ρ, α and v are respectively the density of the fluid, the thermal diffusivity and the kinematic viscosity.

The boundary conditions to be satisfied by the above equations are

$$u = 0, v = 0, T = T_c \quad \text{at } y = H, y = 0, x = H \tag{3.5a}$$
$$u = v = 0 \quad \text{at } x = 0$$

Coupling condition required that the temperature and the heat flux be continuous at the solid fluid interface i.e.

$$\kappa_s \frac{\partial T_{so}}{\partial x} = \kappa_f \left(\frac{\partial T}{\partial x} \right)_{x=0} \tag{3.5b}$$

where κ_s and κ_f are the thermal conductivity of solid and fluid. The temperature T_{so} in the solid as given by Miyamoto et. al [5] is

$$T_{so} = T_H(y) - [T_b - T_H(y)]\frac{x}{b} \tag{3.5c}$$

where $T(y)$ is the unknown temperature at the interface to be determined from the solutions of equations.

3.3 Transformation of the governing equation

The following dimensionless variable are introduced

$$x = \frac{\bar{x}}{L}, \; y = \frac{\bar{y}}{L}, \; u = \frac{\bar{u}}{(\alpha/L)}, \; v = \frac{\bar{v}}{(\alpha/L)}, \; \frac{T-T_c}{T_H - T_c} = \theta, t = \frac{\bar{t}}{(L^2/\alpha)}, \; p = \frac{\bar{p}}{(\rho\alpha^2/L^2)} \tag{3.6}$$

Using the above dimensionless dependent and independent variables in the governing equations (3.1)–(3.4) the following equations are obtained

$$\frac{\partial u}{\partial x} + \frac{\partial v}{\partial y} = 0 \tag{3.7}$$

$$\frac{\partial u}{\partial t} + u\frac{\partial u}{\partial x} + v\frac{\partial u}{\partial y} = -\frac{\partial p}{\partial x} + \Pr\left(\frac{\partial^2 u}{\partial x^2} + \frac{\partial^2 u}{\partial y^2} \right) + \text{Ra}\,\Pr\,\theta\sin\phi \tag{3.8}$$

$$\frac{\partial v}{\partial t} + u\frac{\partial v}{\partial x} + v\frac{\partial v}{\partial y} = -\frac{\partial p}{\partial y} + \Pr\left(\frac{\partial^2 v}{\partial x^2} + \frac{\partial^2 v}{\partial y^2} \right) + \text{Ra}\,\Pr\,\theta\cos\phi \tag{3.9}$$

$$\frac{\partial \theta}{\partial t} + u\frac{\partial \theta}{\partial x} + v\frac{\partial \theta}{\partial y} = \left(\frac{\partial^2 \theta}{\partial x^2} + \frac{\partial^2 \theta}{\partial y^2} \right) \tag{3.10}$$

and boundary condition (3.5a,b,c) transform into

$$u = v = \theta = 0 \text{ at } y = H$$
$$u = v = \theta = 0 \text{ at } y = 0 \tag{3.11}$$
$$u = v = \theta = 0 \text{ at } y = H$$

$$u = v = 0, \quad \theta - 1 = p\frac{\partial\theta}{\partial x} \quad \text{at } x = 0$$

where $B = \overline{B}/L$, $H = \overline{H}/L$, $p = (k/k_s)(b/L)$

where L is reference length and H is the height of the cavity, p is the coupling parameter.

Again equations (3.8) –(3.10) transform into

$$\frac{\partial\Omega}{\partial t} + \frac{\partial(u\Omega)}{\partial x} + \frac{\partial(v\Omega)}{\partial y} = \Pr\nabla^2\Omega + \text{Ra}\,\Pr\left(\cos\phi\frac{\partial\theta}{\partial x} - \sin\phi\frac{\partial\theta}{\partial y}\right) \tag{3.12}$$

$$\frac{\partial\theta}{\partial t} + u\frac{\partial\theta}{\partial x} + v\frac{\partial\theta}{\partial y} = \nabla^2\theta \tag{3.13}$$

where

$$\Omega = -\left(\frac{\partial^2}{\partial x^2} + \frac{\partial^2}{\partial y^2}\right)\psi \tag{3.14}$$

is the vorticity function and ψ is the stream function defined by

$$u = \frac{\partial\psi}{\partial y}, \quad v = -\frac{\partial\psi}{\partial x} \tag{3.15}$$

In the equation (3.12)

$$\text{Ra} = \frac{g\beta(T_b - T_\infty)L^3}{\alpha v} \quad \text{and} \quad \Pr = \frac{v}{\alpha} \tag{3.16}$$

are Rayleigh number and Prandtl number respectively.

Once we know the numerical values of the temperature function we may obtain the rate of heat flux of the walls.

A grid dependence study has been carried out for a thermally driven cavity flow for the above mentioned parameter values with meshes of 31×31, 41×41, 51×51 and 61×61 points and resulting flow quantities are listed in Table 3.1. For computational economy, a 41×41 mesh has been used throughout for the simulations process. With this mesh for the case with $\Pr = 7.0$, $p = 0.0$ and $\text{Ra} = 10^4$ the maximum values of ψ are obtained.

3.4 Method of solution

An upwind finite-difference method, together with successive over relaxaion iteration technique has been employed to integrate the model equations
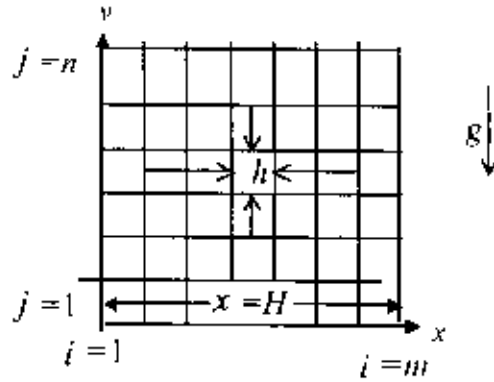

Fig 3.1b. Schematic representation of the cavity depicting the mesh used in the numerical simulations.

(3.12) to (3.14) governing the flow. For computational purposes we first write equations (3.12)-(3.14) to the general form as given below:

$$\frac{\partial F}{\partial t} = -\frac{\partial (UF)}{\partial y} - \frac{\partial (VF)}{\partial y} + A\left\{ \frac{\partial \theta}{\partial x}\cos\phi - \frac{\partial \theta}{\partial y}\sin\phi \right\} + D\left(\frac{\partial^2}{\partial x^2} + \frac{\partial^2}{\partial y^2} \right)F \tag{3.17}$$

Here, F represents either the function Ω or θ and the coefficients A and D are given as follows

$\Omega: \quad A = \text{Ra. Pr}, \quad D = \text{Pr}$

$\theta: \quad A = 0.0, \quad D = 1$ (3.18)

Except for the non-linear terms, all spatial dervatives in the governing differential equation (3.17) are approximated at the interior grid points using second order central difference approximations. Thus we make the following approximations

$$U_{i,j} = \frac{1}{2h}\left(\psi_{i,j+1} - \psi_{i,j-1} \right), \qquad V_{i,j} = -\frac{1}{2h}\left(\psi_{i+1,j} - \psi_{i-1,j} \right) \tag{3.19}$$

and equation (3.15) may also be expressed as

$$\psi_{i,j} = \frac{1}{4}\left(\psi_{i-1,j} + \psi_{i+1,j} + \psi_{i,j-1} + \psi_{i,j+1} \right) + \frac{1}{4}h^2 \Omega_{i,j} \tag{3.20}$$

The successive over-relaxation method represented by the iterative scheme is given below

$$\psi_{i,j}^k = \psi_{i,j} + \frac{\omega}{4}\left(\psi_{i+1,j} + \psi_{i-1,j} + \psi_{i,j+1} + \psi_{i,j-1} - 4\psi_{i,j} - h^2 \Omega_{i,j} \right) \tag{3.21}$$

22

where k is the iteration number, was used to find the stream function from the current vorticity distribution. We used the well-known optimum value of ω given by

$$\omega = \frac{8 - 4\sqrt{4 - \delta^2}}{\delta^2}, \quad \text{where } \delta = \cos\left(\frac{\pi}{m}\right) + \cos\left(\frac{\pi}{n}\right) \tag{3.22}$$

in order to minimize the computational time. In the present computations convergence was assumed when the maximum absolute pointwise change over one iteration was less than 0.0001.

Before we present the discretisation of the nonlinear terms of equation (3.17), we first define U_f and U_b as the average axial velocities evaluated respectively at half a grid forward and backward from point (x_i, y_j) in the x-direction,

$$U_f = \frac{1}{2}\left(U_{i+1,j} + U_{i,j}\right), \qquad U_b = \frac{1}{2}\left(U_{i,j} + U_{i-1,j}\right) \tag{3.23}$$

similarly, we define V_f and V_b

$$V_f = \frac{1}{2}\left(V_{i,j+1} + V_{i,j}\right), \qquad V_b = \frac{1}{2}\left(V_{i,j} + V_{i,j-1}\right) \tag{3.24}$$

As the vertical velocities are averaged half a grid spacing both forward and backward from point (x_i, y_j) in the y-direction respectively, it can easily be verified that the upwind differencing form is automatically preserved when the following numerical formulae are used:

$$\left[\frac{\partial(UF)}{\partial x}\right]_{i,j} = \frac{1}{2h}\left[\left(U_f - |U_f|\right)F_{i+1,j} + \left(U_f + |U_f| - U_b + |U_b|\right)F_{i,j}\right.$$
$$\left. - \left(U_b + |U_b|\right)F_{i-1,j}\right] \tag{3.25}$$

$$\left[\frac{\partial(VF)}{\partial y}\right]_{i,j} = \frac{1}{2h}\left[\left(V_f - |V_f|\right)F_{i,j+1} + \left(V_f + |V_f| - V_b + |V_b|\right)F_{i,j}\right.$$
$$\left. - \left(V_b + |U_b|\right)F_{i,j-1}\right] \tag{3.26}$$

The remaining terms in (3.17) are approximated by using forward differences in time and central differences in space. The individual expressions follow.

$$\left[\frac{\partial F}{\partial t}\right]_{i,j} = \frac{F_{i,j}^{new} - F_{i,j}^{old}}{\Delta t} \tag{2.27}$$

where Δt is the size of time increment and superscript 'new' and 'old' denote the value at the new time $t+\Delta t$ and the earlier time t. Further we have

$$\left(\frac{\partial^2 F}{\partial x^2} + \frac{\partial^2 F}{\partial y^2}\right)_{i,j} = \frac{1}{h^2}\left(F_{i+1,j} + F_{i-1,j} + F_{i,j+1} + F_{i,j-1} - 4F_{i,j}\right) \tag{3.28}$$

$$\left(\frac{\partial\theta}{\partial x}\right)_{i,j} = \frac{1}{2h}\left(\theta_{i+1,j} - \theta_{i-1,j}\right), \quad \left(\frac{\partial\theta}{\partial y}\right)_{i,j} = \frac{1}{2h}\left(\theta_{i,j+1} - \theta_{i,j-1}\right). \tag{3.29}$$

On introducing (3.21)–(3.30) into (3.18) and rearranging the terms we obtain

$$F_{i,j}^{new} = F_{i,j}^{old} + \frac{\Delta t}{2h}\left(-P_1 - P_2 + A(p_4\cos\phi - p_5\sin\phi) + 2D\frac{P_3}{h}\right) \tag{3.30}$$

where

$$P_1 = \left(U_f - |U_f|\right)F_{i+1,j} + \left(U_f + |U_f| - U_b + |U_b|\right)F_{i,j} - \left(U_b + |U_b|\right)F_{i-1,j}, \tag{3.31}$$

$$P_2 = \left(V_f - |V_f|\right)F_{i,j+1} + \left(V_f + |V_f| - V_b + |V_b|\right)F_{i,j} - \left(V_b + |V_b|\right)F_{i,j-1} \tag{3.32}$$

$$P_3 = \left(F_{i+1,j} + F_{i-1,j} + F_{i,j+1} + F_{i,j-1} - 4F_{i,j}\right) \tag{3.33}$$

$$P_4 = \left(\theta_{i+1,j} - \theta_{i-1,j}\right) \tag{3.34}$$

$$P_5 = \left(\theta_{i,j+1} - \theta_{i,j-1}\right) \tag{3.35}$$

Equation (3.30) is used to integrate equation (3.13) at any interior point by replacing the function F by Ω and θ by taking the appropriate coefficients given in (3.18). At any time step the values of Ω and θ are obtained from their respective values at the previous time step, however at the initial instant they are prescribed by the initial conditions. Stream function ψ is calculated based on the vorticity distribution by solving equation (3.15) using the successive over relaxation (SOR) method.

Finally solutions obtained are presented below in terms of streamlines and isotherms. We have allowed the Rayleigh number, Ra to vary from 10^3 to 10^7, the Prandtl number, Pr =7.0, angle of inclination, ϕ is from $0^"$ to 90^0 and coupling parameter, p varies from 0 to 1.

3.5 Results and discussion

Numerical results for natural convection heat transfer for a fluid in an inclined square cavity are studied. As mentioned above, the non-dimensional controlling parameters are the Rayleigh number Ra, the Prandtl number Pr, coupling parameter p and angle of inclination ϕ. In table 3.1 it is seen that the value ψ_{max} gets more accurate as the number of meshes increases.

In Fig. 3.2 we have to first show the streamlines and isotherms for values of p equal to 0.0, 0.25, 0.50, 0.75 and 1.00 for the fixed values of Ra = 10^4, Pr = 7.0 and $\phi = 0^0$. Shape of streamlines are almost same and center of cavity changes for

24

increase of p. The isotherms are clustered at the bottom corner opposite to hot wall of the cavity. Isotherms concentrate hot wall to bottom wall as p increases from 0.0 to 1.0. Tendency to form boundary layer at $p = 1.0$ with bottom cold side of the cavity.

In Fig. 3.3 the calculated flow fields are plotted for angles of inclination ϕ equal to 0^0, 22.50^0, 45^0, 67.50^0 and 90^0 while Ra=10^4, Pr=7.0 and p=0.25. The flow fields are visualized by few stream lines, the associated temperature distribution is plotted for isotherms of $\theta(x, y)$. Streamlines are circular and unicellular in shape. Tendency to form boundary layer from $\phi=67.50^0$ to $\phi=90^0$ in the bottom cold side of the cavity. Flow is concentrated at the right most bottom corner and spreads diagonally to the top most corner in Fig.3.3(b). Isotherms are denser and tendency to form boundary layer at the bottom cold side of the cavity.

. The square cavity shown in Fig. 3.4 is important starting point in the study of flow and heat transfer. The analysis is based on numerical results obtained for values of the Rayleigh numbers in the range from 10^3 to 10^7 while the values of Prandtl number, Pr = 7.0, coupling parameter, $p = 0.25$ and angle of inclination, $\phi=0^0$. With the increase of Rayleigh number Ra the streamlines shape changes. This phenomena is pronounced at Ra=10^7, in main cell the center of which located near lower left corner, the retarded flow form a pocket like structure at Ra=10^5 to 10^7. Isotherms flow condensing from right most cold corner and gradually spreads towards diagoually opposite left most corner as Ra increases from 10^3 to 10^7 and form boundary layer at the bottom and right side of the cavity as Ra increases from 10^5 to 10^7. Also at Ra=10^7 an isolated curve is created in upper side.

In Fig. 3.5 increase of p leads to decrease of heat transfer with the fixed value of Rayleigh number, Ra = 10^4 and Prandtl number, Pr = 7.0.

3.6 Conclusions

Using the Boussinesq approximation and considering buoyancy effects, implicit finite difference technique has been employed. The study have been carried out for a fluid having Prandtl number, $Pr = 7.0$ while the value of the Rayleigh number, Ra varies from 10^3 to 10^7, angle of inclination, ϕ varies from 0^0 to 90^0 and coupling parameter, p varies from 0 to 1. It is observed that the value ψ_{max} gets more accurate as the number of meshes increase.

Table 3.1: Comparison of numerical values of stream function against different meshes for $Ra = 10^4$, $Pr = 7.0$ and $p = 0.0$.

Meshes	$|\Psi_{max}|$
31×31	0.963177
41×41	0.962284
51×51	0.962085
61×61	0.962079

p=0.0

p=0.25

p=0.50

p=0.75

p=1.0

Fig.3.2 (a) Streamlines for different p while Ra=10^4, Pr=7.0 and $\phi=0^0$
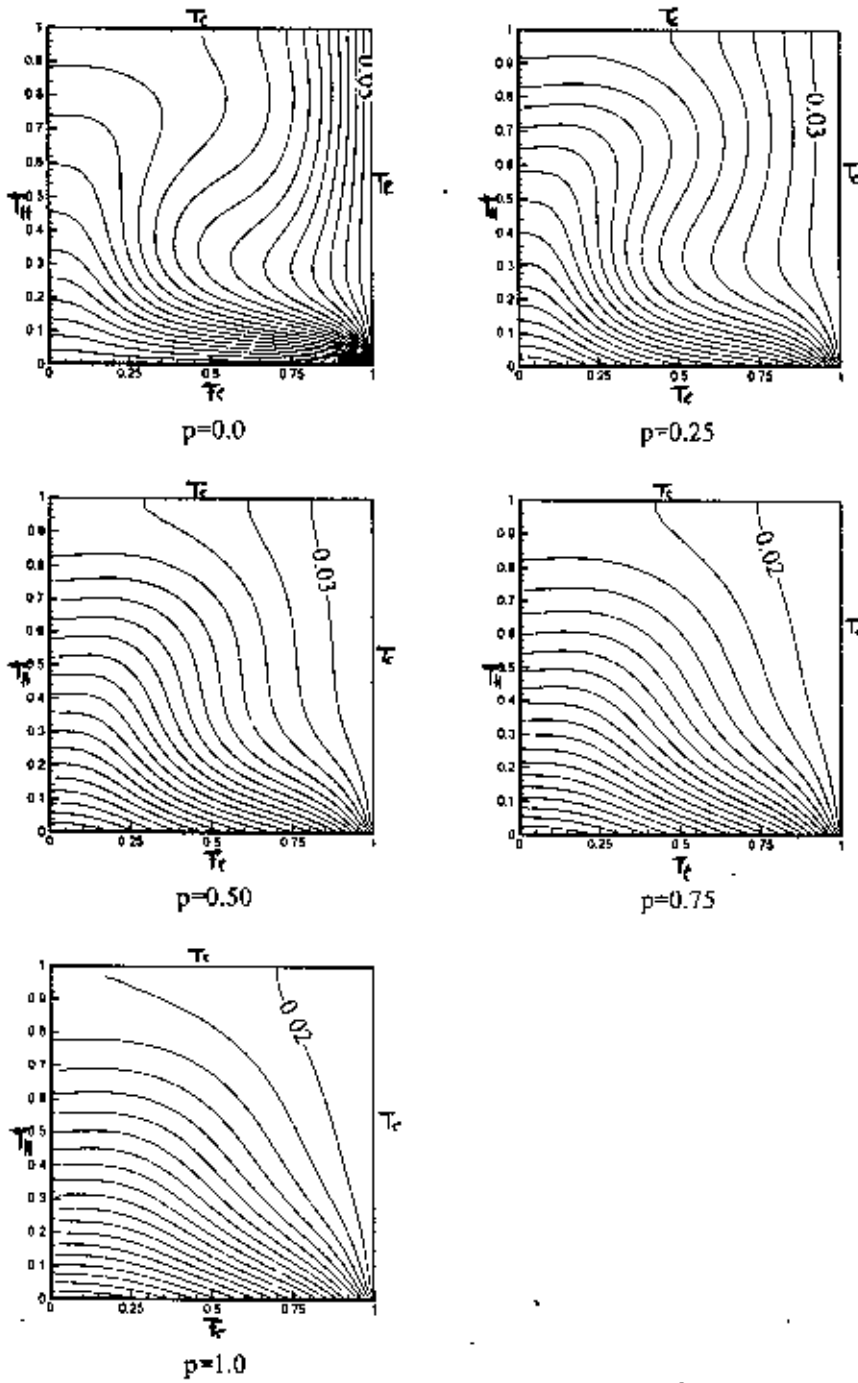
Fig.3.2 (b) Isotherms for different p while Ra=10^4, Pr=7.0 and $\phi=0^0$

$\phi=0^\circ$

$\phi=22.50^\circ$

$\phi=45^\circ$
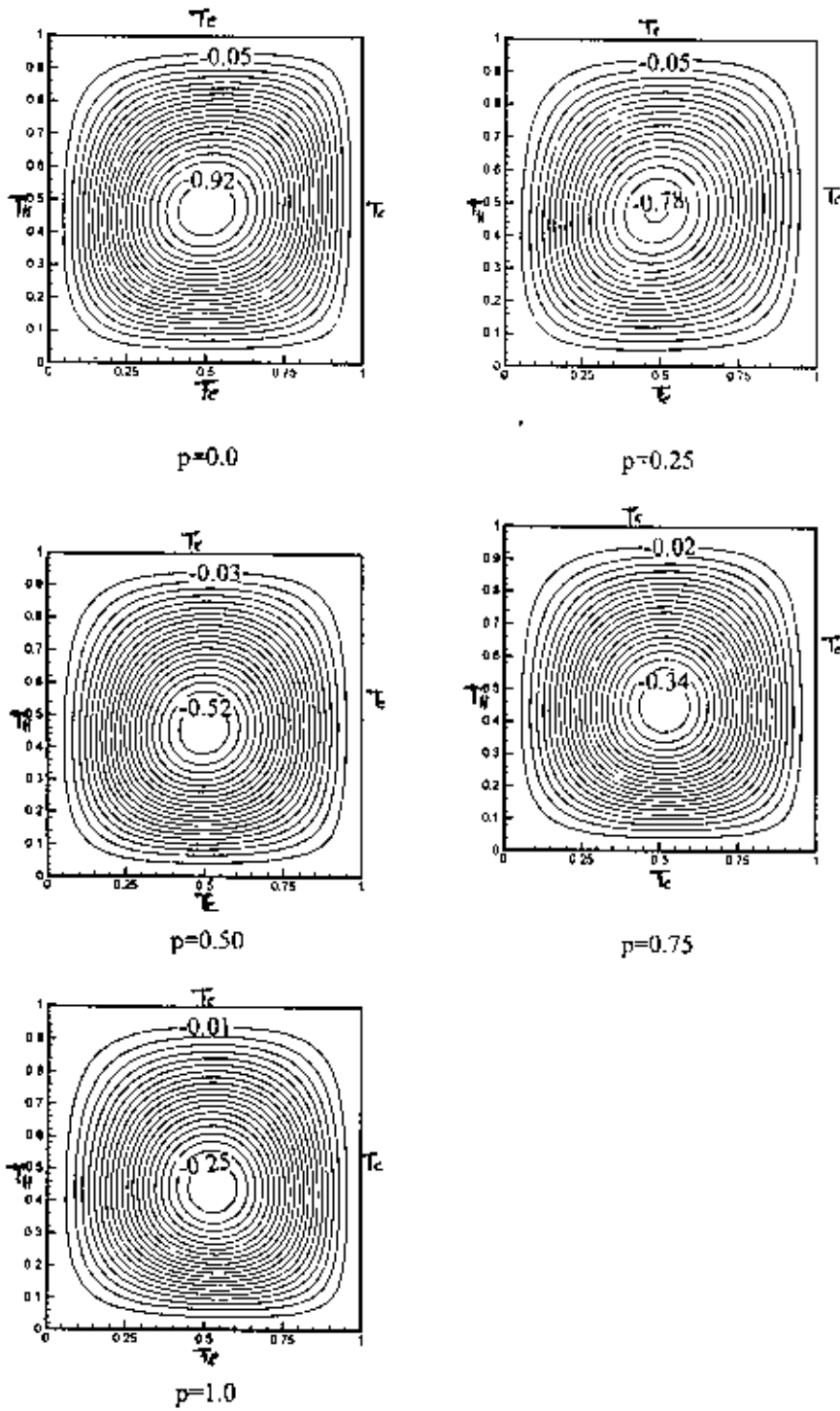
$\phi=67.50^\circ$

$\phi=90^\circ$
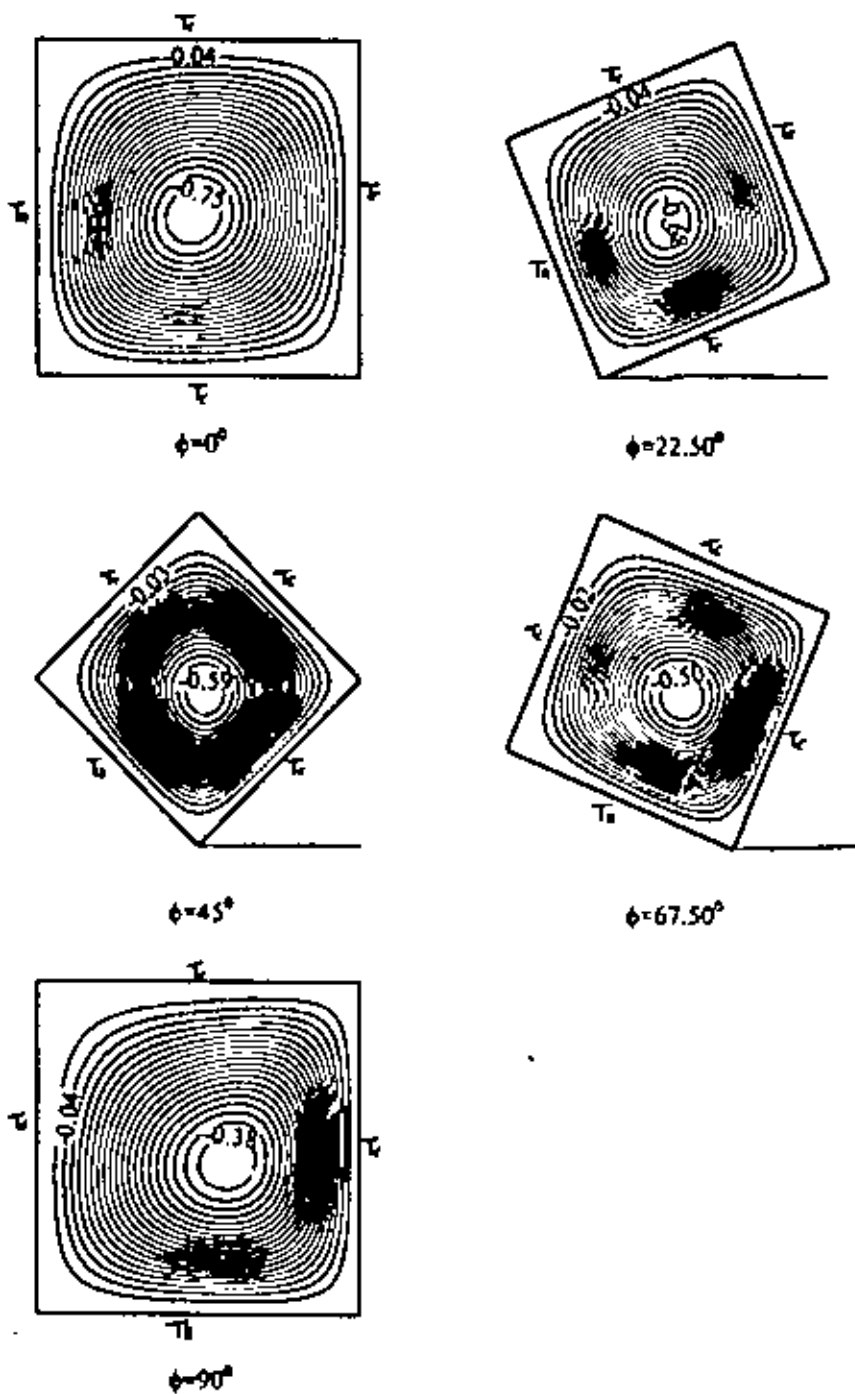
Fig.3.3 (a) Streamlines for different ϕ while Ra=10^4, Pr=7.0 and
p=0.25
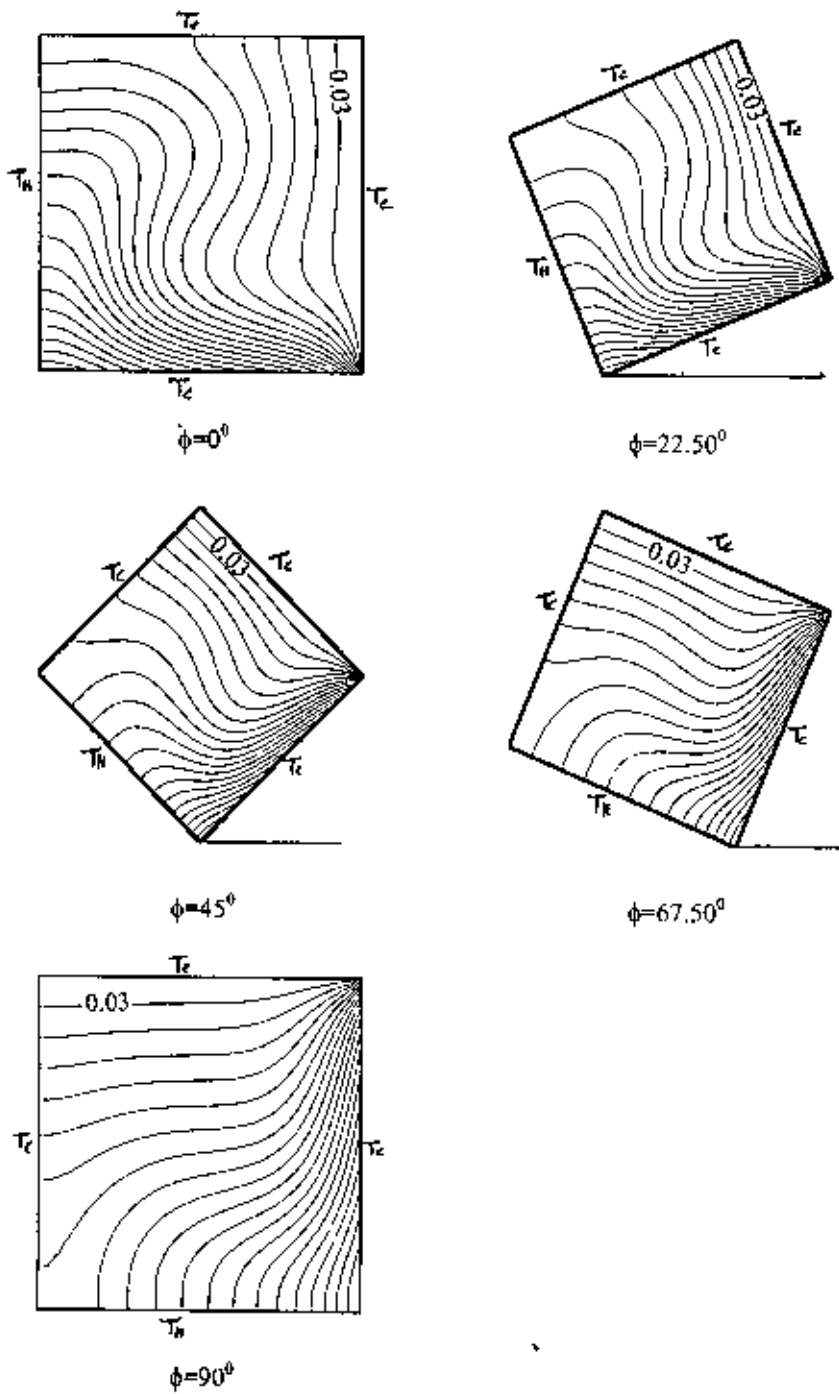
Fig.3.3 (b) Isotherms for different φ while Ra=10⁴, Pr=7.0 and
p=0.25
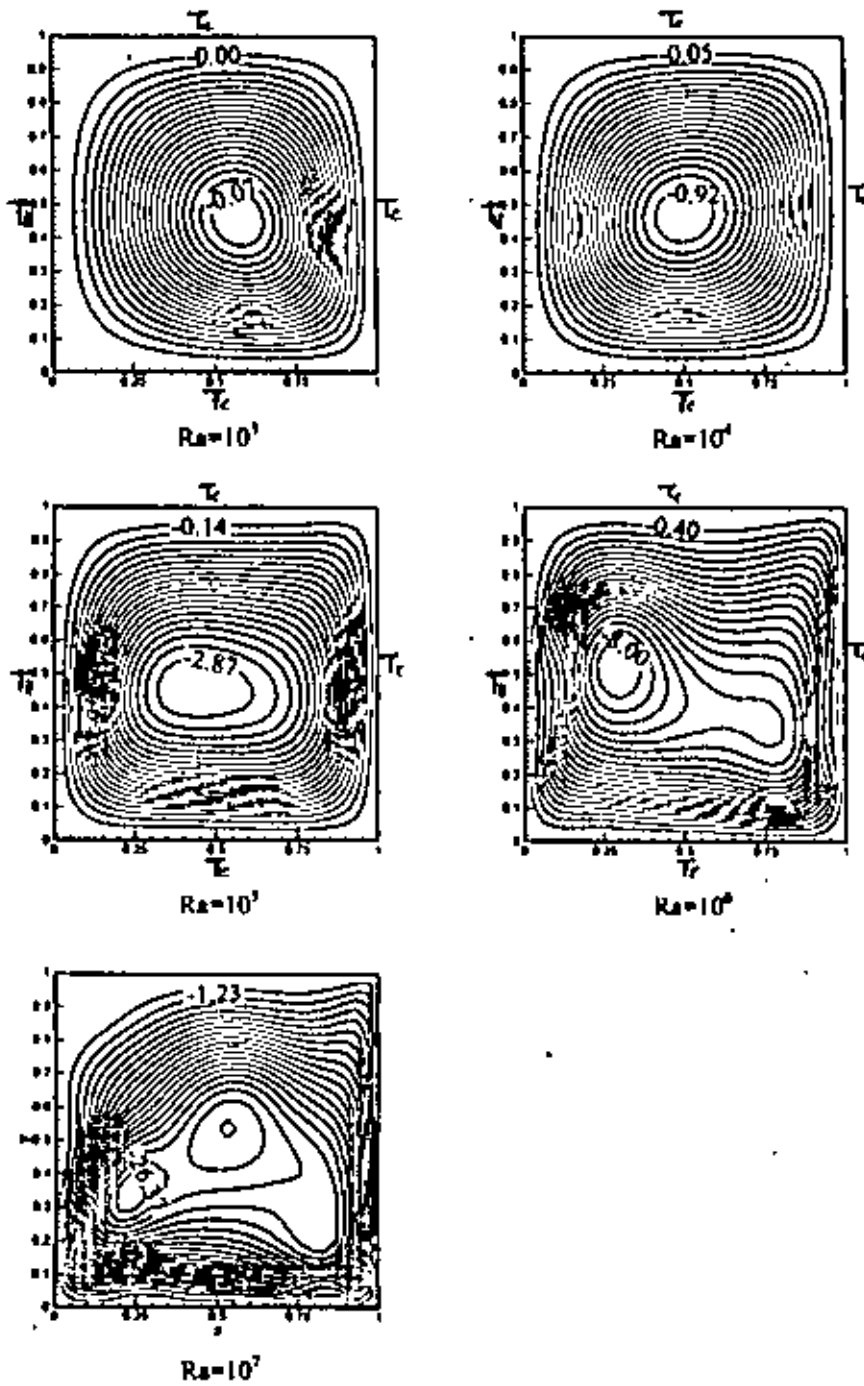
Fig.3.4 (a) Streamlines for different Ra while Pr=7.0, $\phi=0^0$ and
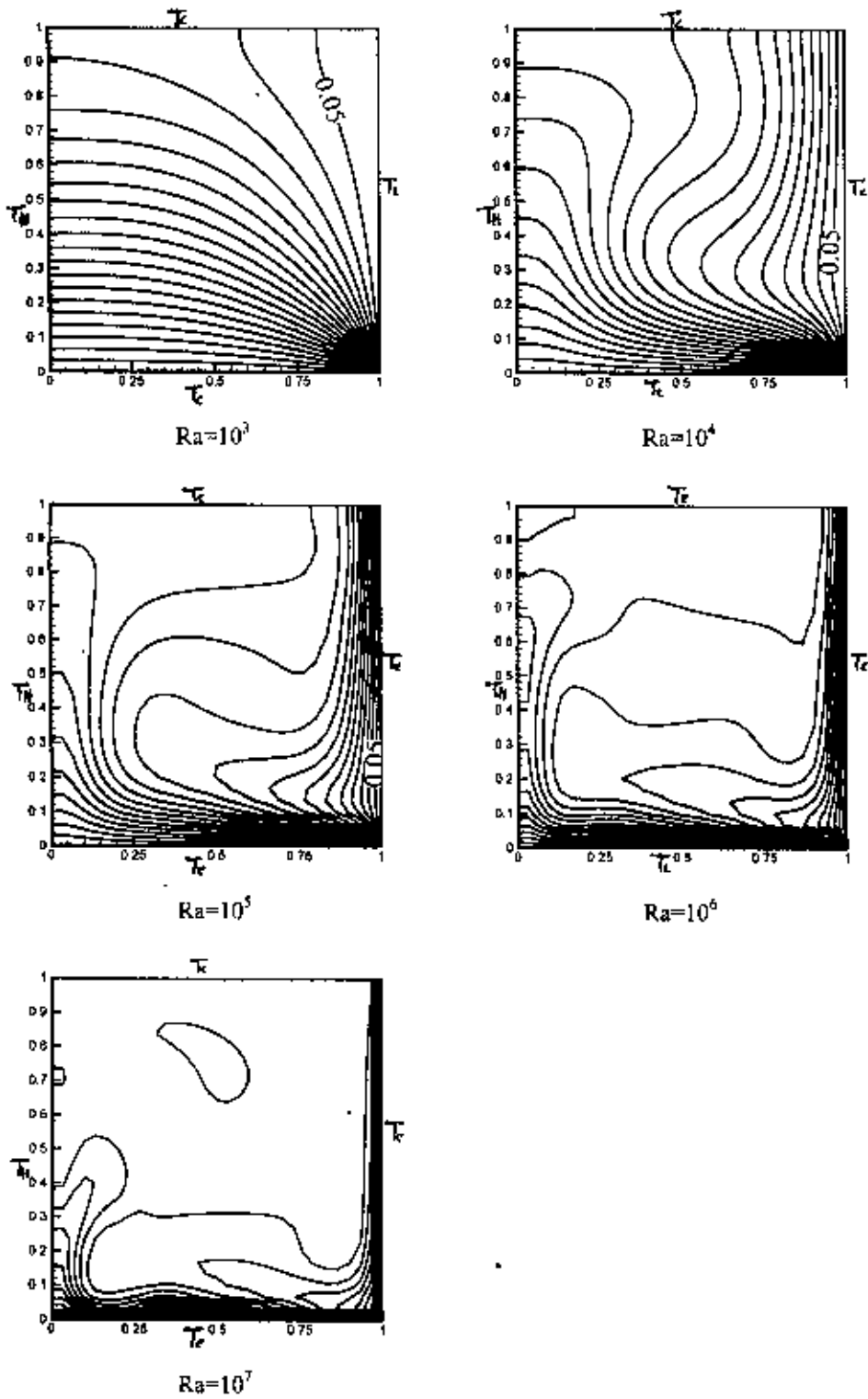$p=0.25$

Ra=10³

Ra=10⁴

Ra=10⁵

Ra=10⁶

Ra=10⁷

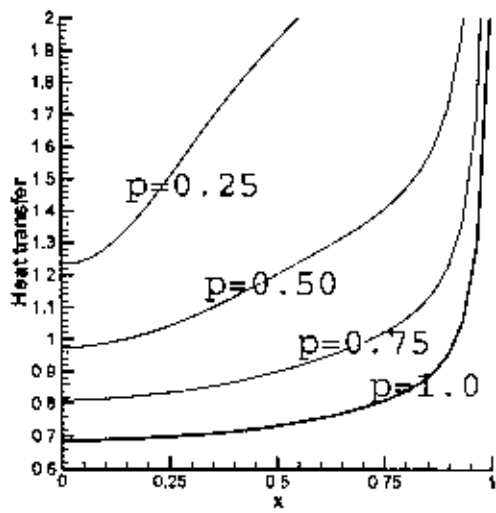Fig.3.4 (b) Isotherms for different Ra while Pr=7.0, $\phi=0^0$ and $p=0.25$

Fig. 3.5 Rate of heat transfer for Pr = 7.0, Ra = 10^4, φ=0.0 and different value of p

Chapter 4

Conclusions

In this thesis, conjugate effect of conduction and convection with natural convection flow from a vertical flat plate and in an inclined square cavity have been investigated. The coupling of conduction required that the temperature and the heat flux be continuous at the interface.

To establish the accuracy of the solution of the present problem two methods, namely the extended series solution and the implicit finite difference method together with Keller-box scheme are employed in Chapter 2.

In Chapter 3, equations are solved numerically by an upwind finite difference method together with a successive over-relaxation (SOR) technique.

The results thus obtained are presented in tabular form (in chapters 2 and 3) for comparison and also graphically in figures (in chapter 2, 3).

From the above observation one can conclude that

1. In Chapter 2 the solutions obtained from the tabular form shows a good agreement. The skin-friction and non-dimensional temperature decreases monotonically as the value of the Prandtl number increases and same as for velocity and temperature profiles.

2. In Chapter 3 numerical results for natural convection heat transfer for a fluid in an inclined square cavity are shown graphically. The streamlines and isotherms for values of p equal to 0.0, 0.25, 0.50, 0.75 and 1.00 for the fixed values of $Ra=10^4$, $Pr=7.0$ are shown. It may be seen that the value ψ_{max} gets more accurate as the number of meshes increases. The region of clustered isotherms moves to the left of the cavity. Shape of streamlines are almost same for increase of p. The calculated flow fields are plotted for angles of inclination of 0^0 to 90^0. The flow fields are visnalized by few streamlines, the associated temperature distribntion is plotted

for isotherms of $\theta(x, y)$. With the increase of Rayleigh number Ra the streamline shape changes and isotherms lines closed to the right, the retarded flow form a pocket like structure at $Ra=10^5$ to 10^7 and form boundary layer at the bottom and right side of the cavity. Also at $Ra=10^7$ an isolated curve is created in upper side. Here increase of p leads to decrease of heat transfer with the fixed value Rayleigh number $Ra = 10^4$, $Pr = 7.0$.

Appendix

Finite difference method

In our analysis, we have employed a number of methods for the numerical solution of the differential equations. Of them the most practical, efficient and accurate solution technique is implicit finite difference method together with Keller-box elimination technique, which is well-documented and widely used by Keller-box and Cebeci [13] and recently by Hossain [9].

Now from equations (2.13)-(2.15) we get

$$f''' + p_1 ff'' - p_2 f'^2 + g = \xi\left(f' \frac{\partial f'}{\partial \xi} - f'' \frac{\partial f}{\partial \xi} \right) \tag{A1}$$

$$\frac{1}{\text{Pr}} g'' + p_1 fg' - p_3 f'g = \xi\left(f' \frac{\partial f'}{\partial \xi} - f'' \frac{\partial f}{\partial \xi} \right) \tag{A2}$$

To apply the aforementioned method, we first convert the equations (A1)-(A2) into the following system of first order equations with dependent variables, $u(\xi, \eta)$, $v(\xi, \eta)$, $p(\xi, \eta)$ as

$$f' = u \tag{A3}$$

$$u' = v \text{ and } g' = p \tag{A4}$$

$$v' + p_1 fv - p_2 u^2 + g = \xi\left(u \frac{\partial u}{\partial \xi} - v \frac{\partial f}{\partial \xi} \right) \tag{A5}$$

$$\frac{1}{\text{Pr}} p' + p_1 fp - p_3 ug = \xi\left(u \frac{\partial g}{\partial \xi} - p \frac{\partial f}{\partial \xi} \right) \tag{A6}$$

where $x = \xi$, $h = g$ and $(16 + 15x)/20(1 + x) = p_1$, $(6 + 5x)/10(1 + x) = p_2$, $1/5(1 + x) = p_3$

and the boundary conditions are

$$f(\xi,0) = 0, \ u(\xi,0) = 0, \ \mathrm{p}(\xi,0) = -(1+\xi)^{1/4} + \xi^{1/5}(1+\xi)^{1/20} g(\xi,0) \qquad \text{(A7)}$$
$$u(\xi,\infty) = 0, g(\xi,\infty) = 0,$$

We now consider the net rectangle on the (ξ,η) plane and denote the net points by

$$\eta_0 = 0, \ \eta_j = \eta_{j-1} + h_j, \ , j = 1,2,\cdots,J$$
$$\xi^0 = 0, \ \xi^n = \xi^{n-1} + k_n, \ , n = 1,2,\cdots,N \qquad \text{(A1)}$$
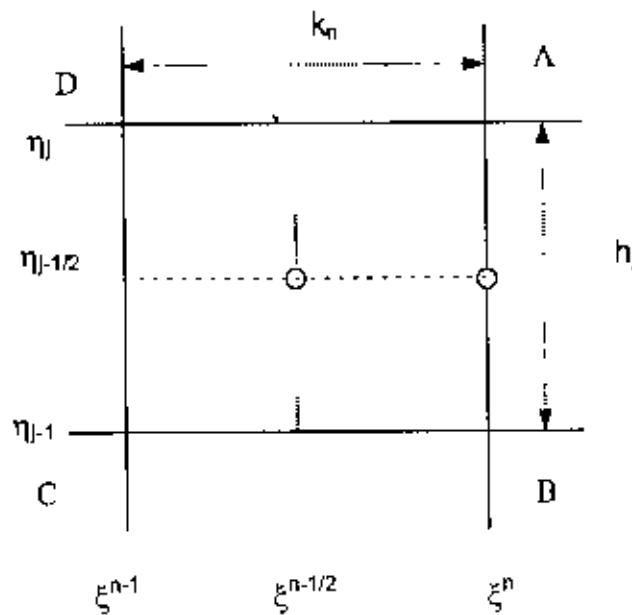
Fig.A Net rectangle of the difference approximation

Here n and j are just sequence of numbers on the (ξ,η) plane, k_n and h_j be the variable mesh widths.

We approximate the quantities f,u,v,g at the point (ξ^n,η_j) of the net by $f_j^n, u_j^n, v_j^n, g_j^n$, which we call net function. We also employed the notation g_j^n for the quantities midway between net points shown in Fig.A and for any net function as

$$\xi^{n-1/2} = \frac{1}{2}(\xi^n + \xi^{n-1}) \qquad \text{(A9)}$$

$$\eta_{j-1/2} = \frac{1}{2}(\eta_j + \eta_{j-1})$$

(A10)

$$g_j^{n-1/2} = \frac{1}{2}(g_j^n + g_j^{n-1})$$

(A11)

$$g_{j-1/2}^n = \frac{1}{2}(g_j^n + g_{j-1}^{n-1})$$

(A12)

Now we write the difference equations that are to approximate equations (A3)-(A6) by considering one mesh rectangle for the mid point $\left(\xi^n, \eta_{j-1/2}\right)$ to obtain

$$\frac{f_j^n - f_{j-1}^n}{h_j} = u_{j-1/2}^n$$

(A13)

$$\frac{u_j^n - u_{j-1}^n}{h_j} = v_{j-1/2}^n$$

(A14)

$$\frac{g_j^n - g_{j-1}^n}{h_j} = p_{j-1/2}^n$$

(A15)

Similarly equations (A5)-(A6) are approximated by centering about the mid point $\left(\xi^{n-1/2}, \eta_{j-1/2}\right)$. Centering the equations (A9) about the point $\left(\xi^{n-1/2}, \eta\right)$ without specifying η to obtain the algebraic equations. The difference approximation to equations (A5)-(A6) become

$$\frac{1}{2}(L^n + L^{n-1}) = \xi^{n-\frac{1}{2}}\left[u^{n-\frac{1}{2}}(\frac{u^n - u^{n-1}}{k_n}) - v^{n-\frac{1}{2}}(\frac{f^n - f^{n-1}}{k_n})\right]$$

(A16)

$$\frac{1}{2}(M^n + M^{n-1}) = \xi^{n-\frac{1}{2}}\left[u^{n-\frac{1}{2}}(\frac{g^n - g^{n-1}}{k_n}) - p^{n-\frac{1}{2}}(\frac{f^n - f^{n-1}}{k_n})\right]$$

(A17)

where

$$L^n = \left[v' + p_1 fv - p_2 u^2 + g\right]^n , \quad L^{n-1} = \left[v' + p_1 fv - p_2 u^2 + g\right]^{n-1}$$

aud

39

$$M^n = \left[\frac{1}{\text{Pr}} p' + p_1 fp - p_3 ug\right]^n \text{ and } M^{n-1} = \left[\frac{1}{\text{Pr}} p' + p_1 fp - p_3 ug\right]^{n-1}$$

$$[v']^n + \alpha_1 (fv)^n - \alpha_2 (u^2)^n + \alpha\left[v^{n-1} f^n - v^n f^{n-1}\right] + g^n = R^{n-1} \tag{A18}$$

$$\frac{1}{\text{Pr}}[p']^n + \alpha_1 (fp)^n - \alpha_3 (ug)^n - \alpha\left[u^{n-1} g^n - u^n g^{n-1}\right.$$
$$\left. + f^{n-1} p^n - f^n p^{n-1}\right] = T^{n-1} \tag{A19}$$

where

$$R^{n-1} = -L^{n-1} + \alpha\left[(fv)^{n-1} - (u^2)^{n-1}\right]$$

$$T^{n-1} = -M^{n-1} + \alpha\left[(fp)^{n-1} - (ug)^{n-1}\right]$$

$$\alpha = \frac{\xi^{n-\frac{1}{2}}}{k_n}, \alpha_1 = p_1 + \alpha, \alpha_2 = p_2 + \alpha, \alpha_3 = p_3 + \alpha$$

Now taking position at $\eta = \eta_{j-\frac{1}{2}}$ then equation (A1)-(A2) become

$$[v']^n_{j-\frac{1}{2}} + \alpha_1 (fv)^n_{j-\frac{1}{2}} - \alpha_2 (u^2)^n_{j-1/2}$$
$$+ \alpha\left[v^{n-1}_{j-\frac{1}{2}} f^n_{j-\frac{1}{2}} - v^n_{j-\frac{1}{2}} f^{n-1}_{j-\frac{1}{2}}\right] + g^n_{j-\frac{1}{2}} = R^{n-1}_{j-\frac{1}{2}} \tag{A20}$$

40

$$\frac{1}{\Pr}\left[p'\right]^{n}_{j-\frac{1}{2}} + \alpha_1\left(fp\right)^{n}_{j-\frac{1}{2}} - \alpha_3\left(ug\right)^{n}_{j-\frac{1}{2}}$$

$$+ \alpha\left[u^{n-1}_{j-\frac{1}{2}} g^{n}_{j-\frac{1}{2}} - u^{n}_{j-\frac{1}{2}} g^{n-1}_{j-\frac{1}{2}} + \right.$$

$$\left. f^{n-1}_{j-\frac{1}{2}} p^{n}_{j-\frac{1}{2}} - f^{n}_{j-\frac{1}{2}} p^{n-1}_{j-\frac{1}{2}} \right]$$

(A21)

where

$$R^{n-1}_{j-\frac{1}{2}} = -L^{n-1}_{j-\frac{1}{2}} + \alpha\left[\left(fv\right)^{n-1}_{j-\frac{1}{2}} - \left(u^2\right)^{n-1}_{j-\frac{1}{2}} \right]$$

$$L^{n-1}_{j-\frac{1}{2}} = h_j^{-1}\left(v_j^{n-1} - v_{j-1}^{n-1}\right) + p_1\left(fv\right)^{n-1}_{j-\frac{1}{2}} - p_2\left(u^2\right)^{n-1}_{j-\frac{1}{2}} + g^{n-1}_{j-\frac{1}{2}}$$

$$T^{n-1}_{j-\frac{1}{2}} = -M^{n-1}_{j-\frac{1}{2}} + \alpha\left[\left(fp\right)^{n-1}_{j-\frac{1}{2}} - \left(ug\right)^{n-1}_{j-\frac{1}{2}} \right]$$

$$M^{n-1}_{j-\frac{1}{2}} = \frac{1}{\Pr} h_j^{-1}\left(v_j^{n-1} - v_{j-1}^{n-1}\right) + p_1\left(fp\right)^{n-1}_{j-\frac{1}{2}} - p_3\left(ug\right)^{n-1}_{j-\frac{1}{2}}$$

Equation (A20) and (A21) become

$$h_j^{-1}\left[v_j^{n} - v_{j-1}^{n}\right] + \alpha_1\left(fv\right)^{n}_{j-\frac{1}{2}} - \alpha_2\left(u^2\right)^{n}_{j-\frac{1}{2}} + g^{n}_{j-\frac{1}{2}}$$

$$+ \alpha\left(v^{n-1}_{j-\frac{1}{2}} f^{n}_{j-\frac{1}{2}} - v^{n}_{j-\frac{1}{2}} f^{n-1}_{j-\frac{1}{2}} \right) = \dot{R}^{n-1}_{j-\frac{1}{2}}$$

(A22)

41

$$\frac{1}{\text{Pr}} h_j^{-1}\left[p_j^n - p_{j-1}^n\right] + \alpha_1 (fp)_{j-\frac{1}{2}}^n - \alpha_3 (ug)_{j-\frac{1}{2}}^n$$

$$+ \alpha\left(u_{j-\frac{1}{2}}^{n-1} g_{j-\frac{1}{2}}^n - u_{j-\frac{1}{2}}^n g_{j-\frac{1}{2}}^{n-1} + f_{j-\frac{1}{2}}^{n-1} p_{j-\frac{1}{2}}^n - f_{j-\frac{1}{2}}^n p_{j-\frac{1}{2}}^{n-1}\right) = T_{j-\frac{1}{2}}^{n-1} \tag{A23}$$

The boundary conditions become

$$f_0^n = 0, \quad u_0^n = 0, \quad p_0^n = -(1+\xi)^{1/4} + \xi^{1/5}(1+\xi)^{1/20} g_0^n \tag{A24}$$

Finally we get

$$h_j^{-1}\left(f_j^n - f_{j-1}^n\right) = u_{j-\frac{1}{2}}^n \tag{A25}$$

$$h_j^{-1}\left(u_j^n - u_{j-1}^n\right) = v_{j-\frac{1}{2}}^n \tag{A26}$$

$$h_j^{-1}\left(v_j^n - v_{j-1}^n\right) + \alpha_1 (fv)_{j-\frac{1}{2}}^n - \alpha_2 (u^2)_{j-\frac{1}{2}}^n + g_{j-\frac{1}{2}}^n$$

$$+ \alpha\left(v_{j-\frac{1}{2}}^{n-1} f_{j-\frac{1}{2}}^n - v_{j-\frac{1}{2}}^n f_{j-\frac{1}{2}}^{n-1}\right) = R_{j-\frac{1}{2}}^{n-1} \tag{A27}$$

$$\frac{1}{\text{Pr}} h_j^{-1}\left[p_j^n - p_{j-1}^n\right] + \alpha_1 (fp)_{j-\frac{1}{2}}^n - \alpha_3 (ug)_{j-\frac{1}{2}}^n$$

$$+ \alpha\left(u_{j-\frac{1}{2}}^{n-1} g_{j-\frac{1}{2}}^n - u_{j-\frac{1}{2}}^n g_{j-\frac{1}{2}}^{n-1} + f_{j-\frac{1}{2}}^{n-1} p_{j-\frac{1}{2}}^n - f_{j-\frac{1}{2}}^n p_{j-\frac{1}{2}}^{n-1}\right) = T_{j-\frac{1}{2}}^{n-1} \tag{A28}$$

We define the iterates

$$\left(f_j^{(i)}, \ u_j^{(i)}, \ v_j^{(i)}, \ g_j^{(i)}\right) \quad j=1,2\ldots$$

with initial values equal to those at the previous ξ station (which is usually the best initial guess variables). For higher iterates we get

$$f_j^{(i+1)} = f_j^{(i)} + \delta f_j^{(i)} \tag{A29}$$

$$u_j^{(i+1)} = u_j^{(i)} + \delta u_j^{(i)} \tag{A30}$$

$$v_j^{(i+1)} = v_j^{(i)} + \delta v_j^{(i)} \tag{A31}$$

$$g_j^{(i+1)} = g_j^{(i)} + \delta g_j^{(i)} \tag{A32}$$

$$p_j^{(i+1)} = p_j^{(i)} + \delta p_j^{(i)} \tag{A33}$$

Now we insert the right hand side of the expression in place of $f_j,\ u_j,\ v_j,\ g_j,$ in equations (A25)-(A28) and drop the terms that are quadratic in

$$\delta f_j^{(i)}, \quad \delta u_j^{(i)}, \quad \delta v_j^{(i)}, \quad \delta g_j^{(i)}$$

to yield the following linear system (for simplicity, the subscript i in δ quantities is dropped)

$$\delta f_j - \delta f_{j-1} - \frac{h_j}{2}\left(\delta u_j + \delta u_{j-1}\right) = \left(r_1\right)_j \tag{A34}$$

$$\delta u_j - \delta u_{j-1} - \frac{h_j}{2}\left(\delta v_j + \delta v_{j-1}\right) = \left(r_4\right)_j \tag{A35}$$

$$\delta g_j - \delta g_{j-1} - \frac{h_j}{2}\left(\delta g_j + \delta g_{j-1}\right) = \left(r_5\right)_j \tag{A36}$$

$$\left(S_1\right)_j \delta v_j + \left(S_2\right)_j \delta v_{j-1} + \left(S_3\right)_j \delta f_j + \left(S_u\right)_j \delta f_{j-1} + \left(S_5\right)_j \delta u_j \tag{A37}$$
$$+ \left(S_6\right)_j \delta u_{j-1} + \left(S_7\right)_j \delta g_j + \left(S_8\right)_j \delta g_{j-1} = \left(r_2\right)_j$$

and

$$(t_1)_j \, \delta p_j + (t_2)_j \, \delta p_{j-1} + (t_3)_j \, \delta f_j + (t_4)_j \, \delta f_{j-1} + (t_5)_j \, \delta u_j$$
$$+ (t_6)_j \, \delta u_{j-1} + (t_7)_j \, \delta g_j + (t_8)_j \, \delta g_{j-1} = (r_3)_j, \tag{A38}$$

where

$$(r_1)_j = f_{j-1}^{(i)} - f_j^{(i)} + h_j u_{j-\frac{1}{2}}^{(i)}$$

$$(r_4)_j = u_{j-1}^{(i)} - u_j^{(i)} + h_j v_{j-\frac{1}{2}}^{(i)}$$

$$(r_5)_j = g_{j-1}^{(i)} - g_j^{(i)} + h_j p_{j-\frac{1}{2}}^{(i)}$$

$$(r_2)_j = R_{j-\frac{1}{2}}^{n-1} - h_j^{-1}\left(v_j^i - v_{j-1}^i\right) - \alpha_1 (fv)_{j-\frac{1}{2}}^i + \alpha_2 \left(u^2\right)_{j-\frac{1}{2}}^i - g_{j-\frac{1}{2}}^i$$

$$- \alpha\left(v_{j-\frac{1}{2}}^{n-1} f_{j-\frac{1}{2}}^i - v_{j-\frac{1}{2}}^i f_{j-\frac{1}{2}}^{n-1} \right)$$

$$(r_3)_j = T_{j-\frac{1}{2}}^{n-1} - \frac{1}{\Pr} h_j^{-1}\left(p_j^i - p_{j-1}^i\right) + \alpha_1 (fp)_{j-\frac{1}{2}}^i - \alpha_3 (ug)_{j-\frac{1}{2}}^i - \alpha(ug)_{j-\frac{1}{2}}^i$$

$$- \alpha\left(u_{j-\frac{1}{2}}^{n-1} g_{j-\frac{1}{2}}^i - u_{j-\frac{1}{2}}^i g_{j-\frac{1}{2}}^{n-1} + f_{j-\frac{1}{2}}^{n-1} p_{j-\frac{1}{2}}^i - f_{j-\frac{1}{2}}^i p_{j-\frac{1}{2}}^{n-1} \right)$$

The coefficients of momentum equation are:

$$(S_1)_j = h_j^{-1} + \frac{\alpha_1}{2} f_j^{(i)} - \frac{\alpha}{2} f_{j-\frac{1}{2}}^{n-1}$$

$$(S_2)_j = -h_{j-1}^i + \frac{\alpha_1}{2} f_{j-1}^{(i)} - \frac{\alpha}{2} f_{j-\frac{1}{2}}^{n-1}$$

$$(S_3)_j = \frac{\alpha_1}{2} v_j^{(i)} + \frac{\alpha}{2} v_{j-\frac{1}{2}}^{n-1}$$

$$(S_4)_j = \frac{\alpha_1}{2} v_{j-1}^{(i)} + \frac{\alpha}{2} v_{j-\frac{1}{2}}^{n-1}$$

$$(S_5)_j = -\alpha_2 u_j^{(i)}$$

$$(S_6)_j = -\alpha_2 u_{j-1}^{(i)}$$

$$(S_7)_j = \frac{1}{2}$$

$$(S_8)_j = \frac{1}{2}$$

The coefficients of energy equation are:

$$(t_1)_j = \frac{1}{\mathrm{Pr}} h_j^{-1} + \frac{\alpha_1}{2} f_j^{(i)} - \frac{\alpha}{2} f_{j-\frac{1}{2}}^{n-1}$$

$$(t_2)_j = -\frac{1}{\mathrm{Pr}} h_{j-1}^j + \frac{\alpha_1}{2} f_{j-1}^{(i)} - \frac{\alpha}{2} f_{j-\frac{1}{2}}^{n-1}$$

$$(t_3)_j = \frac{\alpha_1}{2} p_j^{(i)} + \frac{\alpha}{2} p_{j-\frac{1}{2}}^{n-1}$$

$$(t_4)_j = \frac{\alpha_1}{2} p_{j-1}^{(i)} + \frac{\alpha}{2} p_{j-\frac{1}{2}}^{n-1}$$

$$(t_5)_j = -\frac{\alpha_3}{2} g_j^{(i)} - \frac{\alpha}{2} g_j^i + \frac{\alpha}{2} g_{j-\frac{1}{2}}^{n-1}$$

$$\left(t_6\right)_j = -\frac{\alpha_3}{2}\,g_{j-1}^{(i)} - \frac{\alpha}{2}\,g_{j-1}^{i} + \frac{\alpha}{2}\,g_{j-\frac{1}{2}}^{n-1}$$

$$\left(t_7\right)_j = -\frac{\alpha_3}{2}\,u_{j}^{(i)} - \frac{\alpha}{2}\,u_{j}^{i} - \frac{\alpha}{2}\,u_{j-\frac{1}{2}}^{n-1}$$

$$\left(t_8\right)_j = -\frac{\alpha_3}{2}\,u_{j-1}^{(i)} - \frac{\alpha}{2}\,u_{j-1}^{i} - \frac{\alpha}{2}\,u_{j-\frac{1}{2}}^{n-1}$$

The system of linear equations (A34)-(A38) can be solved in a very efficient manner by using the block-elimination method. Numerical values are obtained from the above technique, results are shown in tabular and graphical form. In table 2.1 and table 2.4, results compare with Pozzi et al [8]. In Fig 2.2 and Fig 2.3, $f''(0, x)$ and $\theta(0, x)$ are shown graphically for comparison with small and large values of x, velocity and temperature profiles are depicted in Fig 2.4 and Fig 2.5 respectively.

References:

[1] L.B.Gdalevich and V.E.Fertman, Conjugate problems of natural convection , *Inzh- Fiz.Zh.* **33** (3),539-547(1977)

[2] M.D.Kelleher and K.T.Yang, A steady conjugate heat transfer problem with conduction and free convection , *Appl. Scient.Res.* 17, 240-268 (1967)

[3] G.S.H.Lock and J.C.Gunn, Laminar free convection from a downward projecting fin, *J. Heat Transfer* **90**,63-70 (1968)

[4] K.Chida and Y.Katto, steady on conjugate heat transfer by vectorial dimensional analysis, *Int.J.Heat Mass Transfer* **10**, 453-460 (1976).

[5] M. Miyamoto , J. Sumikawa, T. Akiyoshi and T. Nakamura : Effect of axial heat conduction in a vertical flat plate on free convection heat transfer . *Int. J. Heat Mass Transfer* **23**, 1545-1533 (1980).

[6] J. Timma et J. P. Padet, Etude theorique du couplage convection conduction en convection libre laminaire surune plaque verticale, *Int. J. Heat Mass Transfer* **28**, 1097-1104 (1985).

[7] J. Gosse, Analyse simplifiee du couplage conduction convection pour un ecoulement a couche limite laminaire sur uneplaque plane, *Rev. Gen. Therm.* **228**, 967 (1980).

[8] Pozzi and M. Lupo,The coupling of conduction with laminar natural convection along a flat plate, *Int. J. Heat Mass Transfer* **31**, No. 9. pp. 1807-1814 (1988)

[9] Hossain, M. A. , Banu, N., Nakayama, A. Non-Darcy forced convection boundary layer flow over a flat plate embedded in a saturated porous media. *Num Heat Transfer.* **26**, 399-414 (1994)

[10] Sparrow, E. M. and Gregg, J. L., Laminar free convection from a vertical flat plate with Uniform Surface Heat Flux, *Tran. ASME,* vol. 78, pp. 435-440 (1956)

[11] Pohlhausen, E. Dr Warmeaustausch Zwischen Korpen Und Flussigkeiten mit Kleiner Reiburg and Kleiner Warmeleitung, *Z. Angew. Math. Mech.,* Vol. 1, p. 115, (1911)

[12] Schmidt, E. , and Beckmann, W. , Das Temperatur und Geschwindig klitsfeld Von einer warme Abgebenden Senkrechten platte bei naturlicher Konvektian, *Forsch-Ing.-Weg.*, vol. 1, p. 391, (1930)

[13] Cebeci, T. and Bradshow, P. , *Momentum Transfer in Boundary Layers*, McGraw-Hill Book Company (1977).

[14] Nachtsheim. P.R. and Swigert, P. Satisfaction of asymptotic boundary conditions in numerical solution of systems of non-linear equation of boundary layer type *NASA TN D*-3004 (1965).

[15] Loyd, J. R. and Sparrow, E. M. : Combined forced and free convection flow on vertical surface, *Int. J. Heat Mass Transfer* 13, pp. 434-438 (1970)

[16] Shiralkar, G. and Tien, C. (1982), A Numerical study of the effect of a vertical temperature difference imposed on a horizontal enclosure, *Numerical Heat Transfer*, Vol. 5. pp. 185-197.

[17] Chao, P. and Ozoe, H. (1983), Laminar natural convection in an inclined rectangular box with lower surface half-heated and half insulated, *ASME J. Heat Transfer*, Vol. 105, pp. 425-432.

[18] Anderson, R. and Lauriat, G. (1986) The horizontal natural convection boundary layer regime in a closed cavity, *Proc. 8th Int. Heat Transfer Conf.*, San Francisco, California, USA, pp. 1453-1458.

[19] Kimura, S. and Bejan, A., (1985), Natural convection in differentially heated corner region, *Physics Fluids*, Vol. 28, pp. 2980-2989.

[20] November, M. and Nansteel, M. W., (1987), Natural convection in a rectangular enclosure heated from below and cooled along one surface, *Int. J. Heat Mass Transfer*, Vol. 30, pp. 2433-2440.

[21] Nicolas, J. D. and Nansteel, M. W. (1993), Natural convection in a rectangular enclosure with partial heating on the lower surface; experimental results, *Int. J. Heat Mass Transfer*, Vol. 36, pp. 4067-4071.

[22] Ganzarolli, M. M. and Milanez, L. F., (1995). Natural convection in rectangular enclosures heated from below and symmetrically cooled from the sides, *Int. J. Heat Mass Transfer*, Vol. 38, pp. 1063-1073

[23] Velusamy, K., Sundarajan, T. and Seetharamn, K. N., (1998), Laminar natural convection in an enclosure formed by non-isothermal walls, *Proc.of 11th Int. Conf. Heat Transfer*, Korea, Vol. 3, pp. 459-464.

[24] Vafai, K. and Tien, C. L. (1981), Boundary and inertia effects on flow and heat transfer in porous media, *Int. J. Heat Mass Transfer*, Vol. 24, pp. 195-203.

[25] Khanafer, K. M. and Chamkha, A. J. (1999) Mixed convection flow in a lid-driven enclosure filled with a fluid-saturated porous media, *Int. J. Heat Mass Transfer*, vol. 42, pp. 2465-2481.

[26] Patankar, S. V., (1980), *Numerical Heat Transfer and Fluid Flow*, Hemisphere, Washington, DC.

[27] M. A. Hossain and D. A. S. Rees, (2000), Natural convection flow of a viscous incompressible fluid in a rectangular porous medium cavity heated from below(submitted)